

Optimal Experimental Design for Universal Differential Equations

Christoph Plate^{1,2}

Carl Julius Martensen¹

Sebastian Sager¹

¹Otto von Guericke University Magdeburg

{carl.martensen, christoph.plate, sager}@ovgu.de

²Max Planck Institute for Dynamics of Complex Technical Systems Magdeburg

{plate}@mpi-magdeburg.mpg.de

August 15, 2024

Abstract

Complex dynamic systems are typically either modeled using expert knowledge in the form of differential equations, or via data-driven universal approximation models such as artificial neural networks (ANN). While the first approach has advantages with respect to interpretability, transparency, data-efficiency, and extrapolation, the second approach is able to learn completely unknown functional relations from data and may result in models that can be evaluated more efficiently. To combine the complementary advantages, universal differential equations (UDE) have been suggested, which replace unknown terms in the differential equations with ANN. These hybrid models allow to both encode prior domain knowledge such as first principles and to learn unknown mechanisms from data. Often, data for the training of UDE can only be obtained via costly experiments. We consider optimal experimental design (OED) for the planning of experiments and generation of data needed to train UDE. The number of weights in the embedded ANN usually leads to an overfitting of the regression problem. To make the OED problem tractable for optimization, we propose and compare dimension reduction methods that are based on lumping of weights and singular value decomposition of the Fisher information matrix (FIM), respectively. They result in lower-dimensional variational differential equations which are easier to solve and which yield regular FIM. Our numerical results showcase the advantages of OED for UDE, such as an increased data-efficiency and better extrapolation properties.

1 Introduction

Model identification and usage. Chemical engineering has been successfully using concepts from modeling, simulation, and optimization for many decades. Depending on particular applications, optimization has been used for different model-based design and control purposes [87]. The focus was either on descent-based nonlinear programming for single-objective optimization [9], derivative-free algorithms for multi-objective optimization [21], stable and efficient control concepts [23], or on mixed-integer programming, e.g., in superstructure optimization [60]. In most parts of the extensive literature on process optimization, the underlying mathematical models have been derived from domain knowledge and consisted of systems of differential equations for transient processes, or of algebraic equations for (assumed) steady states. Shortcomings in the modeling process have been accounted for by methods from uncertainty quantification and robust optimization. The emergence of powerful data-driven universal approximation models is about to bring a revolution to the field, with many opportunities for research breakthroughs in the intersection of chemical engineering and machine learning [81]. Designing mathematical models and training them has matured over the last decades. Especially for particular machine learning tasks, such as the training of large language models or image processing models, impressive improvements could be achieved. The situation is different, though, in the context of chemical engineering, due to comparatively sparse and expensive-to-observe data and challenging multi-scale modeling tasks with unknown functional relations. In addition, chemical engineering simulation and optimization tasks are typically computationally expensive. Surrogate models for process optimization are surveyed with respect to accuracy and computational effort in [62].

Relevant for many processes with partially unknown mechanisms is thus model identification [11, 14], the symbolic reconstruction of equations from data (and thus different from system identification). A number of different frameworks have been considered in the literature, including grammar-based methods, sparse regression, neural networks, Gaussian process regression, Bayesian approaches, and symbolic regression [35, 11, 25, 14, 61]. Symbolic regression can, e.g., be based on the sparse identification of nonlinear dynamics (SINDy) algorithm [12, 55], genetic algorithms [74], or mixed-integer optimization [18, 45, 7, 2]. Yet, there are many open research questions in model discovery and because of the numerical challenges of inferring symbolic expressions from data, often an intermediate training of a hybrid model is favorable [57].

Universal differential equations. Because of this, we think that combining data-driven surrogate models and differential equations is a very promising approach. The relationship between differential equations and neural networks has been studied in several papers. E.g., it is well known that residual ANN can be interpreted as explicit Euler discretizations of ordinary differential equations (ODE) [39]. Also, several approaches have been suggested how the two concepts can be combined in hybrid models. In addition to structure-based methods, such as physics-informed, Hamiltonian, and Lagrangian neural networks (PINN, HNN, LNN respectively) [70], hybrid models that combine a first-principle model with an embedded machine learning model are of particular interest. A notable example is the framework of universal differential equations (UDE) [69]. Unlike PINNs, HNNs and LNNs, this approach uses automatic differentiation through the underlying numerical solver of the differential equation, allowing efficient training of the surrogates. With the universal approximation theorem, ANN are known to approximate continuous functions on compact sets to any desired accuracy, if they are large enough and use discriminatory activation functions [20, 42]. Consequently, embedding them in differential equation models results in a trainable model capable of learning aspects of the underlying dynamics, assuming sufficient data quality and an appropriate network architecture. Training these universal approximators within the differential equation entails a) differentiating the solution of the differential equation with respect to the neural network parameters, typically achieved via the adjoint method as discussed in [69], and b) updating the parameters using this information, e.g., by employing a variant of steepest descent or stochastic gradient methods like Adam [46]. To formally introduce UDE, assume we have a standard ordinary differential equation (ODE) initial value problem on a fixed time horizon $\mathcal{T} = [0, t_f]$

$$\dot{x}(t) = f(x(t), u(t), p), \quad x(0) = x_0(p) \quad (1)$$

with parameters $p \in \mathbb{R}^{n_p}$ and sufficiently smooth right-hand side function $f : \mathbb{R}^{n_x} \times \mathbb{R}^{n_u} \times \mathbb{R}^{n_p} \mapsto \mathbb{R}^{n_x}$ and controls $u \in \mathcal{U}$. Now, the right-hand side function f may be comprised of three parts: First, a function $\hat{f} : \mathbb{R}^{n_x} \times \mathbb{R}^{n_u} \times \mathbb{R}^{n_{\hat{p}}} \mapsto \mathbb{R}^{n_{\hat{f}}}$, whose structure is known a-priori from domain knowledge (e.g., from first-principles) and which may contain parameters $\hat{p} \in \mathbb{R}^{n_{\hat{p}}}$, e.g., physical constants. Second, a universal approximator model $U : \mathbb{R}^{n_x} \times \mathbb{R}^{n_{\theta}} \mapsto \mathbb{R}^{n_U}$ with parameters $\theta \in \mathbb{R}^{n_{\theta}}$ that may capture unknown parts of the model. Third, a function $f_S : \mathbb{R}^{n_{\hat{f}}} \times \mathbb{R}^{n_U} \mapsto \mathbb{R}^{n_x}$ which represents the composition of the known and unknown parts of the UDE. With $p = (\hat{p}, \theta)$, the initial values $x(0) = x_0(\hat{p})$ are independent of θ and the right-hand side is

$$f(x(t), u(t), p) = f_S \left(\hat{f}(x(t), u(t), \hat{p}), U(x(t), \theta) \right) \quad (2)$$

i.e., the function \hat{f} is complemented by an ANN, e.g., as a replacement of a submodel. The ANN itself has $J \in \mathbb{N}$ layers. As a reminder, in the simplest case each of these layers consists of a linear transformation composed with a (typically nonlinear) activation function that is applied elementwise, i.e.,

$$x^{(j)} = s^{(j)} \left(W_j x^{(j-1)} + b_j \right), \quad j \in [J]. \quad (3)$$

Here, $x^{(0)} = x(t)$ is the input to the feed-forward ANN, $W_j \in \mathbb{R}^{d_j \times d_{j-1}}, b_j \in \mathbb{R}^{d_j}$ are the weights and biases, $s^{(j)}$ the activation function and $d_j \in \mathbb{N}$ the dimension of the j -th layer, respectively. We denote with $\theta^{(j)} = \text{vec}(W_j, b_j) \in \mathbb{R}^{d_j \cdot (d_{j-1} + 1)}$ the weights and biases of the j -th layer stacked together as one vector and with $\theta = \cup_{j \in [J]} \theta^{(j)} \in \mathbb{R}^{n_{\theta}}$ the weights and biases of all layers. Our prediction function U is simply given by

$$U(x(t), \theta) = x^{(J)}. \quad (4)$$

Note that this formal definition also allows without loss of generality to consider several ANN at once by simply stacking the different output vectors in a slightly modified definition (4).

With this, the parameters p of our model comprise a) the weights and biases $\theta \in \mathbb{R}^{n_\theta}$ of the embedded ANN and b) the model parameters \hat{p} of the first-principle model \hat{f} . Note that a generalization towards partial differential algebraic equations on the one hand, and towards more involved ANN topologies can be done in a similar, straightforward way. We restrict ourselves to the case of UDE composed of ODE and feed-forward ANN mainly in the interest of notational simplicity.

UDEs as a hybrid model between differential equations and data-driven universal approximators as suggested in [69, 36, 44] have been applied in areas as diverse as chemical engineering [58], glacier ice flow modeling [10], modeling of COVID-19 regional transmission [75], neuroscience [28], climate modeling [34, 71], hydrology [40], and pharmacology [86]. Using the general definition (2) from above, UDEs contain the important special cases of ODEs (i.e., no embedded ANN) and of neural ODEs [15] (i.e., no domain knowledge in \hat{f}) as often used for theoretical studies, e.g., to investigate lifted approaches [24] or connections to optimal control theory and the turnpike phenomenon [76].

Active learning and optimal experimental design. Experimental training data may be sparse and difficult to obtain in domains like chemical engineering. Designing information-rich experiments has been studied for the two extreme cases of UDEs mentioned above: the training of ANNs and the parameter estimation in differential equations. In the first case, the machine learning community uses the approaches and terminology of *active learning*, in the second case the statistical approach *optimal experimental design* is often preferred. Active learning is a large and very active research field. While it is intuitively clear that regions of the training domain where the model behaves highly nonlinear should be preferred to select training samples, it is challenging to design algorithms that do this automatically. There are several contributions on how to select training samples for ANN or other surrogate models, see, e.g., [16, 82, 26] for a general introduction to active learning and further references, [73] for a survey focussing on deep learning, [66] for a critical study of the effectiveness of active learning, [31] for connections to reinforcement learning, and [22] for connections to Bayesian Optimization. Also, in the context of model order reduction the concept of active learning has been applied successfully [6, 36, 37, 92].

Learning model parameters for differential equations is traditionally related to the statistical approach of optimal experimental design (OED). OED is a systematic approach for obtaining useful data for parameter estimation, model identification, and model discrimination. The estimated model parameters as solutions of, e.g., maximum likelihood estimation problems, are random variables, and are hence endowed with confidence regions. How a process is controlled and when and what is being measured, have an important impact on the size of this confidence regions. OED optimizes controls and sampling decisions in the sense of minimizing the size of this confidence region, as discussed in several textbooks [32, 1, 67, 47]. See, e.g. [49, 77, 79, 90, 72, 13], for an extension of the concept to dynamic systems (ODEs) and applications in chemical engineering.

The online version of OED is conceptually closely related to (online) active learning and data assimilation. In sequential OED, experimental designs are calculated, experimental data obtained, and model parameters estimated iteratively [50, 53]. Sequential OED has been extended by online OED in which the experiment is directly re-designed when a new measurement is taken [84, 33, 4, 68, 54]. OED has also been applied in the context of dual control, in which sequentially an optimal control, experimental design, and parameter estimation problems are solved [43] or exploration versus exploitation is balanced using policy gradients [83]. While some software solutions for OED of dynamic systems have been published, e.g., [59, 90], there are no general purpose methods available to treat complex differential equation models. Furthermore, designing optimal experiments for the concurrent estimation of model parameters of a differential equation and the weight vectors of embedded submodels is completely open. While there are some contributions for the training of ANN using OED [17, 19, 56], our paper is to our knowledge the first that proposes OED for UDE, especially with the ansatz to formulate and solve OED as a specifically structured mixed-integer optimal control problem, as suggested in [77].

Ill-posed inverse problems and dimension reduction. Ill-posed OED problems have been discussed in the literature [3, 91]. A variety of approaches have been proposed to overcome the issue of structural and practical non-identifiability, which corresponds to non-invertible or ill-conditioned matrices. Popular are truncated singular value decomposition (SVD) and column subset selection [29], which can be seen as special cases of model order reduction [5]. They are based on identifying lower-dimensional approximations

of relevant matrices. A particular challenge is the determination of the threshold value for truncating SVD [30] with interesting suggestions such as the L-curve approach [91]. We will have a look at truncated SVD in the context of UDEs, where due to the typical overparametrization of ANN the ill-posedness is not the exception, but the typical situation.

Contributions and outline. The paper is organized as follows. We start with some definitions and by formulating the OED problem for ODE as an optimal control problem in Section 2. In Section 3 we apply this setting to the case of UDE and discuss ways to reduce the computational complexity. Numerical results for benchmark problems are presented in Section 4 that illustrate the advantages of this approach when compared to equidistant sampling of longitudinal data. We conclude with a discussion in Section 5.

2 Optimal experimental design as an optimal control problem

For models described by ODEs, the OED problem can be formulated as a specifically structured mixed-integer optimal control problem (MIOCP) [77]. A variety of different approaches has been suggested for OED, e.g., formulations based on the variance-covariance matrix of the linearized model or robust formulations [51], sigma points or other approaches allowing to calculate approximations of global sensitivities [79], polynomial chaos [85], Gaussian process surrogates [64], adaptive discretizations [80], nonlinear preconditioners [63], transport maps [52], or Bayesian optimization [38]. While we think that the proposed methodology for UDE of the following section can be applied to most of these approaches in a more or less straightforward way, we focus here on the linearized variant of OED.

In this approach, we add the so-called sensitivities $G = dx/dp$ of the states x with respect to the model parameters p to the system (1) of differential equations. The variational differential equations (VDE) for $G = dx/dp : [0, t_f] \mapsto \mathbb{R}^{n_x \times n_p}$ can be derived by taking derivatives of the system solution

$$x(t) = x_0 + \int_0^t f(x(t), u(t), p) dt$$

with respect to time t and parameters p , resulting in the matrix-valued ODE initial value problem

$$\dot{G}(t) = f_x(x(t), u(t), p)G(t) + f_p(x(t), u(t), p), \quad G(0) = \frac{\partial x_0}{\partial p}. \quad (5)$$

Here, f_x and f_p denote the partial derivatives of f with respect to x and p . Note that usually only a subset of all parameters is included here, while others are considered to be known and fixed. Without loss of generality, such fixed constants can be considered as part of the function f . With the sensitivities, also the FIM $F(t_f)$ and its inverse, the variance-covariance matrix $F(t_f)^{-1}$ of the linearized least squares parameter estimation problem, can be modeled in the control problem. The goal of OED is to reduce the volume of the ellipsoid associated with the variance-covariance matrix. Because matrices can not be totally ordered, the experimental design community defined a variety of scalar objective functions $\phi : \mathbb{R}^{n_p \times n_p} \mapsto \mathbb{R}$. Typical examples are the trace (A-criterion and weighted sum of half-axes), $\phi_A(F(t_f)) = \frac{1}{n_p} \text{tr}(F(t_f)^{-1})$, the determinant (D-criterion and proxy for the volume), $\phi_D(F(t_f)) = \det(F(t_f)^{-1})^{\frac{1}{n_p}}$, and the maximal eigenvalue (E-criterion and maximal half-axis), $\phi_E(F(t_f)) = \max\{\lambda : \lambda \text{ is eigenvalue of } F(t_f)^{-1}\}$. The degrees of freedom of the OED problem involve initial values x_0 , control functions u to excite the system, and sampling functions (when and what to measure) w . The OED problem for 1 formulated as a MIOCP is

$$\begin{aligned} \min_{x, x_0, G, F, z, w, u} \quad & \phi(F(t_f)) \\ \text{s.t.} \quad & \dot{x}(t) = f(x(t), u(t), p) \\ & \dot{G}(t) = f_x(x(t), u(t), p)G(t) + f_p(x(t), u(t), p), \\ & \dot{F}(t) = \sum_{i=1}^{n_y} w_i(t)(h_x^i(x(t))G(t))^\top (h_x^i(x(t))G(t)), \\ & \dot{z}(t) = w(t), \\ & x(0) = x_0, \quad G(0) = \frac{\partial x_0}{\partial p}, \quad F(0) = 0, \quad z(0) = 0, \\ & u(t) \in \mathcal{U}, \\ & w(t) \in \mathcal{W}, \\ & z_i(t_f) \leq M_i, \end{aligned} \quad (\text{OED})$$

with (differential) states $x(t) : \mathcal{T} \mapsto \mathbb{R}^{n_x}$ and their initial condition $x_0 \in \mathbb{R}^{n_x}$, model parameters $p \in \mathbb{R}^{n_p}$, time $t \in \mathcal{T}$, and controls $u(t) : \mathcal{T} \mapsto \mathbb{R}^{n_u}$. In addition to 1 we also require an observed function $y = h(x)$ with $h : \mathbb{R}^{n_x} \mapsto \mathbb{R}^{n_y}$ and $y : \mathcal{T} \mapsto \mathbb{R}^{n_y}$. The first and second constraint in (OED) denote the time evolution of the dynamical system and of the sensitivities $G : \mathcal{T} \mapsto \mathbb{R}^{n_x \times n_p}$ of x with respect to p , respectively. The evolution of the symmetric matrix $F : \mathcal{T} \mapsto \mathbb{R}^{n_p \times n_p}$ is given by the weighted sum of observability gramians $h_x^i(x(t)) G(t)$, $i = 1, \dots, n_y$ for each observed function of states. The weights $w_i(t) \in \{0, 1\}$, $i = 1, \dots, n_y$ are the (binary) sampling decisions, where $w_i(t) = 1$ denotes the decision to perform a measurement at time t . The objective $\phi(F(t_f))$ of Mayer type is a suitable OED criterion as discussed above. In this formulation, upper bounds M_i are provided as maximum amounts (in continuous time) of measurements. See [77] for a detailed discussion of discrete-time and continuous-time measurements in OED, alternative formulations penalizing measurements in the objective function (with a hyperparameter that models the trade-off between information gain and experimental costs of measurements), and a detailed analysis of solution structures.

The special features of (OED) with respect to standard optimal control problems, such as the non-dependency of some differential states (x) on others (G and F), the inverse in the objective function, the integrality of sampling functions, or the positive-semidefiniteness of the right hand-side of \dot{F} , can and should be exploited in efficient algorithms and software [51, 77, 90, 59].

A pretty straightforward result will become useful later, when the dimension of sensitivities shall be reduced.

Lemma 1. *Let a well-posed VDE (5) with (x, u, p) be given and let $G(\cdot)$ be a solution. Let $A \in \mathbb{R}^{n_p \times n_A}$ be a matrix. Then the solution $G_s : [0, t_f] \mapsto \mathbb{R}^{n_x \times n_A}$ of the VDE*

$$\dot{G}_A(t) = f_x(x(t), u(t), p)G_A(t) + f_p(x(t), u(t), p)A, \quad G_A(0) = \frac{\partial x_0}{\partial p}A \quad (6)$$

exists uniquely and is given by

$$G_A(t) = G(t)A. \quad (7)$$

Proof. Unique existence follows from the Picard-Lindelöf theorem, multiplication with A does not affect the Lipschitz continuity of f_x and f_p implied by the assumed well-posedness. That $G_A(t) = G(t)A$ is a solution of (6) can be seen by multiplying (5) with A from the right-hand side and using $\dot{G}_A = (\dot{G}A) = \dot{G}A$. \square

3 The extension towards universal differential equations

We consider OED problems of type (OED) for UDE of type (2). The combined parameter estimation and training problem involves model parameters $\hat{p} \in \mathbb{R}^{n_{\hat{p}}}$ and weights and biases $\theta \in \mathbb{R}^{n_{\theta}}$ of the embedded ANN. Qualitatively, they can both be captured in one large vector $p \in \mathbb{R}^{n_p}$ without any changes to the setting of (OED). Quantitatively, though, the number n_{θ} of weights θ is typically very large in comparison to the number of model parameters \hat{p} . This poses two main issues: First, also the number of variational differential equations for the sensitivities $G(\cdot)$ is very large, resulting in a drastic increase of computation time. Second, ANN are often overparametrized. This structural and practical non-identifiability of the weights leads to singular Fisher information matrices (FIM), violating a major assumption of OED contrasting it to most methods from active learning which are typically based on some kind of space-filling sampling of the training domain. The challenge in our setting, where we are interested in experimental designs for the estimation of both kinds of parameters, \hat{p} and θ , is thus to find ways to reduce the dimension of G and hence of the FIM $F(t_f)$ such that the approximation of the FIM is invertible, accurate, and comparatively fast-to-evaluate.

3.1 Dimension reduction methods

In OED optimization problems, one fixes all free parameters p to an initial guess \bar{p} that serves as a linearization point of the nonlinear model. The follow-up parameter estimation of p with new experimental data is only accounted for by taking sensitivities with respect to p into account via the VDE (5). This implies that the general approach is still valid, if model evaluations based on \bar{p} are combined with a reduced number or

approximations of sensitivities. We propose and investigate three particular approaches to do this and hence overcome the issue of overfitting in the context of OED.

Lumping of all weights, (OED-NN-I). The first approach to obtain regular FIM $F(t_f)$ when dealing with equations of type (2) is to introduce one single dummy parameter $p_l = 1.0$ for the embedded ANN with which all n_θ weights and biases are formally multiplied, i.e.,

$$\theta_l = \theta \cdot p_l =: \Xi_l \cdot p_l \quad (8)$$

with $\Xi_l := \theta \in \mathbb{R}^{n_\theta}$. Thus, p_l can be interpreted as a proxy for capturing the overall influence of all weights and biases as it is propagated through the network U during inference, similar to a model parameter multiplied to a known and fixed algebraic term in the right hand side. While the sensitivities with respect to this artificial parameter are different in dimension and value from the sensitivities with respect to the weights of the ANN, resulting experimental designs might still be a good choice. As a major advantage, for one embedded ANN this approach reduces the dimension of the variational differential equations $G_l : \mathcal{T} \mapsto \mathbb{R}^{n_x \times 1}$ and of the FIM $F_l(t_f) \in \mathbb{R}^{1 \times 1}$ drastically. We denote this approach for problem (OED) as (OED-NN-I).

Layerwise lumping of weights, (OED-NN-II). Taking this idea a step further, we introduce scaling parameters for subsets of weights and biases. However, it is not clear a priori how these subsets should be chosen to obtain regular FIM that can be used in the framework of (OED). A natural heuristic choice is to scale the weights and biases of each layer $j \in [J]$, thereby capturing the influence of each layer on the overall dynamics. Formally this can be done by introducing a vector of parameters $p_{ll} = [1.0, \dots, 1.0] \in \mathbb{R}^J$ with elements that are formally multiplied to the weights and biases of the individual layers of the ANN,

$$\theta_{ll} = [\theta \odot \mathbb{1}_{\theta_i \in \theta^{(1)} \forall i \in [n_\theta]}, \dots, \theta \odot \mathbb{1}_{\theta_i \in \theta^{(J)} \forall i \in [n_\theta]}] \cdot p_{ll} =: \Xi_{ll} \cdot p_{ll}, \quad (9)$$

where \odot denotes the Hadamard product of element-wise multiplication and $\Xi_{ll} \in \mathbb{R}^{n_\theta \times J}$. The entries of Ξ_{ll} are hence given by

$$\Xi_{ll,i,j} = \begin{cases} \theta_i, & \text{if } \theta_i \text{ belongs to layer } j, \text{ for } i \in [n_\theta], j \in [J] \\ 0, & \text{otherwise} \end{cases}$$

This approach yields sensitivities $G_{ll}(\cdot) \in \mathbb{R}^{n_x \times J}$ and a FIM $F_{ll}(t_f) \in \mathbb{R}^{J \times J}$ and will be referred to as (OED-NN-II) in the following.

Singular value decomposition, (OED-NN-SVD- n_s). Motivated by reduced-order modeling approaches [5] and previous application in OED [3], we propose to use the truncated singular value decomposition (SVD) of the FIM to select the most relevant weights and biases. The basic idea is to compute the SVD of the FIM using the VDE (5) for G_c and then truncating the SVD with the n_s largest singular values, with $n_s \ll n_\theta$. The relevant weights and biases can be determined by identifying the nonzero elements in the corresponding singular vectors. Only these enter the VDE in (OED), to which we shall refer to as (OED-NN-SVD- n_s)).

Illustration for prototypical example. Figure 1 illustrates the sensitivities G_c, G_l, G_{ll} , and G_{SVD} for an ANN $U(x(t), \theta)$ embedded in the Lotka Volterra equations $\dot{x}_1(t) = x_1(t) - U(x(t), \theta) - \hat{p}_2 u(t) x_1(t)$ and $\dot{x}_2(t) = -x_2(t) + U(x(t), \theta) - \hat{p}_4 u(t) x_2(t)$, see also Section 4.2. The ANN $U(x(t), \theta)$ for the interaction term in $n_x = 2$ differential states has $J = 4$ layers, $n_\theta = 81$ weights, and different nonlinear activation functions. Shown are sensitivities for the $n_s = 2$ largest singular values. The sensitivities thus map \mathcal{T} to $\mathbb{R}^{2 \times 81}, \mathbb{R}^{2 \times 1}, \mathbb{R}^{2 \times 4}$, and $\mathbb{R}^{2 \times 2}$, respectively. The different dimensions indicate the potential of dimension reduction in terms of computational speedup.

Figure 2 shows the corresponding FIM. Here one observes the potential of dimension reduction in terms of regularity of the FIM.

Note that many other dimension reduction approaches are possible. For example, instead of (OED-NN-I) with $U(x(t), p_l \theta)$, one could also consider the sensitivities of $p_l U(x(t), \theta)$. This formulation is not as nicely related to the other formulations as shall become apparent in the next section, though, and hence not further considered.

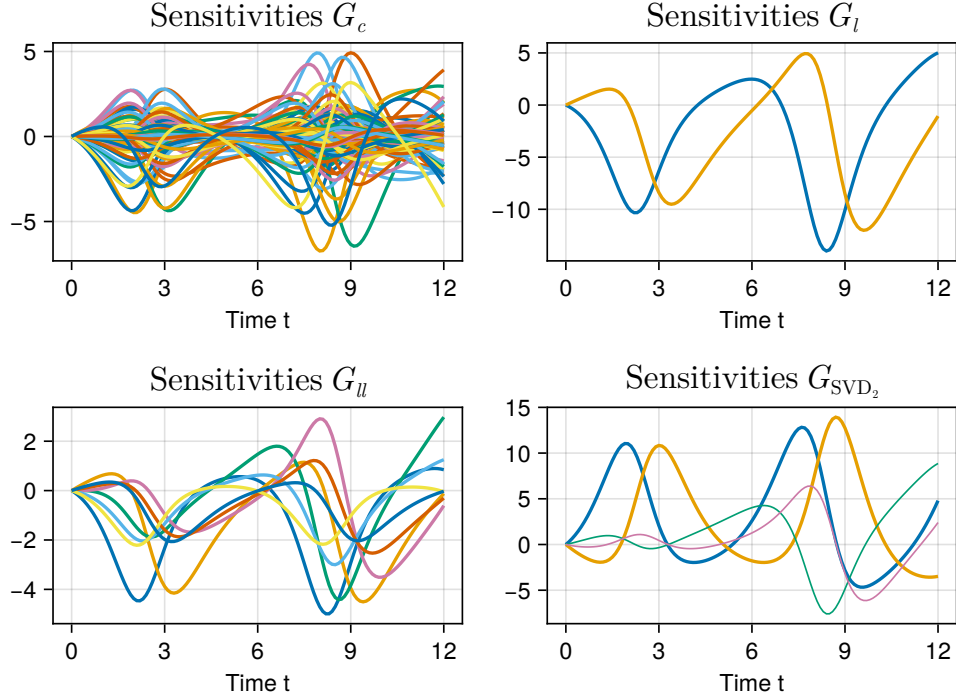


Figure 1: Illustration of sensitivities for ANN embedded in the Lotka-Volterra equations. Although they have different dimensions, the time intervals of interest (those with high absolute values) are similar.

3.2 Calculation of sensitivities and Fisher information matrix

After the conceptual introduction of the different approaches to reduce the dimension, we have a closer look at how the sensitivities can be calculated and how they are related among another. For the block matrix sensitivities $G(t) = [G_{\hat{p}}(t) \ G_c(t)]$ of the differential states x with respect to all parameters $p = (\hat{p}, \theta)$ application of the general VDE (5) and of the particular UDE structure (2) yields

$$\frac{d}{dt} [G_{\hat{p}}(t) \ G_c(t)] = \frac{\partial f}{\partial x}(x(t), u(t), p) [G_{\hat{p}}(t) \ G_c(t)] + \frac{\partial f}{\partial p}(x(t), u(t), p) \quad (10)$$

$$= \left(\frac{\partial f_S}{\partial \hat{f}} \frac{\partial \hat{f}}{\partial x} + \frac{\partial f_S}{\partial U} \frac{\partial U}{\partial x} \right) [G_{\hat{p}}(t) \ G_c(t)] + \left[\frac{\partial f_S}{\partial \hat{f}} \frac{\partial \hat{f}}{\partial \hat{p}} \ \frac{\partial f_S}{\partial U} \frac{\partial U}{\partial \theta} \right] \quad (11)$$

with initial values $G_{\hat{p}}(0) = dx(0)/d\hat{p} \in \mathbb{R}^{n_x \times n_{\hat{p}}}$ and $G_c(0) = \mathbf{0} \in \mathbb{R}^{n_x \times n_{\theta}}$. Note that we omitted arguments in (11) for notational simplicity. Formulation (11) generalizes pure first-principle models with $\partial_U f_S = 0, \partial_{\hat{f}} f_S = 1$ and neural ordinary differential equations with $\partial_U f_S = 1, \partial_{\hat{f}} f_S = 0$. The (usually ill-posed) problem (OED) of computing designs to accurately estimate θ will be denoted as (OED-NN-c).

Integrating the third differential equation in (OED) for the particular case of (2) gives the FIM

$$F(t_f) = \begin{pmatrix} F_{\hat{p}\hat{p}} & F_{\hat{p}c} \\ F_{\hat{p}c}^T & F_{cc} \end{pmatrix} (t_f) \quad (12)$$

$$:= \begin{pmatrix} \int_0^{t_f} \sum_{i=1}^{n_y} w_i(t) G_{\hat{p}}^T(t) h_x^{iT}(x(t)) h_x^i(x(t)) G_{\hat{p}}(t) & \int_0^{t_f} \sum_{i=1}^{n_y} w_i(t) G_{\hat{p}}^T(t) h_x^{iT}(x(t)) h_x^i(x(t)) G_c(t) \\ \int_0^{t_f} \sum_{i=1}^{n_y} w_i(t) G_c^T(t) h_x^{iT}(x(t)) h_x^i(x(t)) G_{\hat{p}}(t) & \int_0^{t_f} \sum_{i=1}^{n_y} w_i(t) G_c^T(t) h_x^{iT}(x(t)) h_x^i(x(t)) G_c(t) \end{pmatrix} dt \quad (13)$$

Using the notation from above, we obtain the following result for the weight lumping approaches.

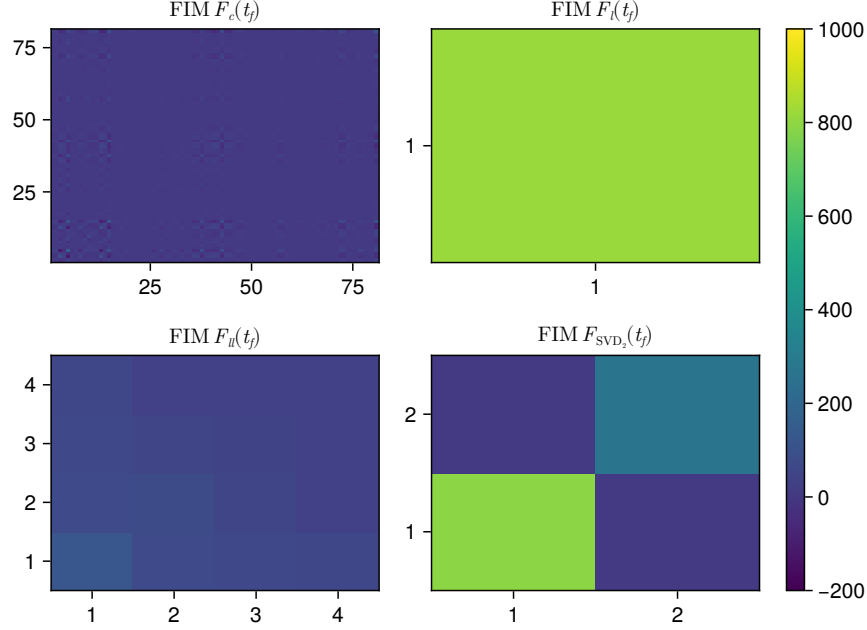


Figure 2: Comparison of FIM $F(t_f)$ corresponding to the sensitivities from Figure 1. The FIM is indefinite for (OED-NN-c), but positive definite for the other approaches.

Lemma 2. Let $U : \mathbb{R}^{n_x} \times \mathbb{R}^{n_\theta} \mapsto \mathbb{R}^{n_{\hat{x}}}$ be an ANN with weights $\theta \in \mathbb{R}^{n_\theta}$. Let Ξ_l and Ξ_u be defined as in (8) and (9), respectively, and $\mathbb{1}_J$ be the all ones vector of dimension J . Then for t almost everywhere in \mathcal{T}

$$G_l(t) = G_c(t) \cdot \Xi_l, \quad (14)$$

$$G_u(t) = G_c(t) \cdot \Xi_u, \quad (15)$$

$$G_l(t) = G_u(t) \cdot \mathbb{1}_J. \quad (16)$$

Proof. We start by looking at the VDE (11) derived above. We observe that f_x , $\frac{\partial f_s}{\partial f} \frac{\partial \hat{f}}{\partial \hat{p}}$ and $\frac{\partial f_s}{\partial U}$ are independent of the particular approach (OED-NN-c) (OED-NN-l), and (OED-NN-ll)). Application of the chain rule for the setting $p_l = 1.0$ and $\theta_l = \theta \cdot p_l$ yields

$$\begin{aligned} \frac{\partial U}{\partial p_l}(x(t), \theta_l) &= \frac{\partial U}{\partial \theta}(x(t), \theta_l) \cdot \frac{\partial \theta_l}{\partial p_l} \\ &= \frac{\partial U}{\partial \theta}(x(t), \theta) \cdot \theta \\ &= \frac{\partial U}{\partial \theta}(x(t), \theta) \cdot \Xi_l. \end{aligned}$$

Therefore and with the trivial property $G_l(0) = \mathbf{0} = G_c(0) \cdot \Xi_l$, we can apply Lemma 1 with the choice $A = \Xi_l = \theta \in \mathbb{R}^{n_\theta \times 1}$ and obtain equation (14).

Equation (15) follows similarly for the setting $p_u = [1.0, \dots, 1.0] \in \mathbb{R}^J$ and $\theta_u = \Xi_u \cdot p_u$ via

$$\frac{\partial U}{\partial p_u}(x(t), \theta_u) = \frac{\partial U}{\partial \theta}(x(t), \theta_u) \cdot \frac{\partial \theta_u}{\partial p_u} = \frac{\partial U}{\partial \theta}(x(t), \theta) \cdot \Xi_u$$

with $\Xi_u \in \mathbb{R}^{n_x \times J}$. Equation (16) follows from $\Xi_l = \Xi_u \mathbb{1}_J$. □

The relations between the corresponding FIM follow directly.

Corollary 3. *With the notation from above for (OED-NN-c) (OED-NN-l), and (OED-NN-ll) we have*

$$F_l(t_f) = \begin{pmatrix} I & 0 \\ 0 & \Xi_l \end{pmatrix}^T F(t_f) \begin{pmatrix} I & 0 \\ 0 & \Xi_l \end{pmatrix} \quad (17)$$

$$F_{ll}(t_f) = \begin{pmatrix} I & 0 \\ 0 & \Xi_{ll} \end{pmatrix}^T F(t_f) \begin{pmatrix} I & 0 \\ 0 & \Xi_{ll} \end{pmatrix} \quad (18)$$

Proof. Follows from multiplication using $F(t_f)$ from (13) as

$$\begin{pmatrix} I & 0 \\ 0 & \Xi_l \end{pmatrix}^T F(t_f) \begin{pmatrix} I & 0 \\ 0 & \Xi_l \end{pmatrix} = \begin{pmatrix} I & 0 \\ 0 & \Xi_l \end{pmatrix}^T \begin{pmatrix} F_{\hat{p}\hat{p}} & F_{\hat{p}c} \\ F_{\hat{p}c}^T & F_{cc} \end{pmatrix} \begin{pmatrix} I & 0 \\ 0 & \Xi_l \end{pmatrix} = \begin{pmatrix} F_{\hat{p}\hat{p}} & F_{\hat{p}c}\Xi_l \\ \Xi_l^T F_{\hat{p}c}^T & \Xi_l^T F_{cc}\Xi_l \end{pmatrix}$$

and comparing the result to inserting (14) in the definition of the FIM. The argument is identical for (18). \square

We now consider approximations of sensitivities and FIM in the SVD approach.

Lemma 4. *Let $U : \mathbb{R}^{n_x} \times \mathbb{R}^{n_\theta} \mapsto \mathbb{R}^{n_{\hat{x}}}$ be an ANN with weights $\theta \in \mathbb{R}^{n_\theta}$. Then there exists for any number $1 \leq n_s \leq n_\theta$ of positive singular values of $F_{cc}(t_f)$ a matrix $V \in \mathbb{R}^{n_\theta \times n_s}$ such that*

$$F_{SVD_{n_s}}(t_f) = \begin{pmatrix} I & 0 \\ 0 & V \end{pmatrix}^T F(t_f) \begin{pmatrix} I & 0 \\ 0 & V \end{pmatrix} = \begin{pmatrix} F_{\hat{p}\hat{p}} & F_{\hat{p}c}V \\ V^T F_{\hat{p}c}^T & D \end{pmatrix} \quad (19)$$

where $D = V^T F_{cc} V \in \mathbb{R}^{n_s \times n_s}$ is a diagonal, positive definite matrix with eigenvalues of $F_{cc}(t_f)$ on the main diagonal. Additionally, we have for t almost everywhere in \mathcal{T}

$$G_{SVD_{n_s}}(t) = G_c(t) \cdot V. \quad (20)$$

Proof. We consider the decomposition of the lower right submatrix $F_{cc}(t_f)$ of $F(t_f)$

$$F_{cc}(t_f) = \int_0^{t_f} \sum_{i=1}^{n_y} (h_x^i(x(t))G_c(t))^T (h_x^i(x(t))G_c(t)) dt = \hat{U} \hat{D} \hat{V}^T \quad (21)$$

with $\hat{U}, \hat{V} \in \mathbb{R}^{n_\theta \times n_\theta}$ unitary matrices and $\hat{D} \in \mathbb{R}^{n_\theta \times n_\theta}$ diagonal containing the singular values of $F_{cc}(t_f)$. As $F_{cc}(t_f)$ is symmetric and positive semidefinite by construction, $\hat{U} = \hat{V}$ can be chosen, and, moreover, singular values and eigenvalues of $F_{cc}(t_f)$ coincide [41, Corollary 2.5.11]. We obtain

$$\begin{aligned} \hat{D} &= \hat{V}^T F_{cc}(t_f) \hat{V} \\ &= \hat{V}^T \sum_{i=1}^{n_y} \int_0^{t_f} (h_x^i(x(t))G_c(t))^T (h_x^i(x(t))G_c(t)) dt \hat{V} \\ &= \sum_{i=1}^{n_y} \int_0^{t_f} (h_x^i(x(t))G_c(t) \hat{V})^T (h_x^i(x(t))G_c(t) \hat{V}) dt \end{aligned} \quad (22)$$

Truncating the singular value decomposition (21) and replacing \hat{V} in (22) by $V \in \mathbb{R}^{n_\theta \times n_s}$, where V is given by the columns of \hat{V} corresponding to the n_s largest singular values of $F_{cc}(t_f)$, we can obtain a lower-dimensional, diagonal, and positive definite approximation $D \in \mathbb{R}^{n_s \times n_s}$ of $F_{cc}(t_f)$:

$$D = \sum_{i=1}^{n_y} \int_0^{t_f} (h_x^i(x(t))G_c(t)V)^T (h_x^i(x(t))G_c(t)V) dt \quad (23)$$

The term $G_c(t)V$ can be interpreted as reduced sensitivities $G_{SVD_{n_s}}(t) \in \mathbb{R}^{n_x \times n_s}$. Property (20) follows from Lemma 1, similarly to the proof argument in Lemma 2. \square

The approximation of $F_{cc}(t_f)$ with a diagonal matrix containing the n_s largest eigenvalues is particularly interesting, because the A-, D-, and E-criteria for the objective $\phi(F(t_f))$ of (OED) mentioned in Section 2 can be formulated in terms of eigenvalues. This follows from basic linear algebra results, such as the trace being the sum of all eigenvalues, the determinant being the product of all eigenvalues, and the eigenvalues of an inverse matrix A^{-1} being the inverse of those of the matrix A . Also, singular value decompositions are known to provide the best rank- n_s approximation of a matrix in the Frobenius norm [27]. As (w, u, x, G, F, z) change during optimization, for fixed matrices V the expression $(\sum_{i=1}^{n_y} \int_0^{t_f} (h_x^i(x(t))G_c(t)V)^T (h_x^i(x(t))G_c(t)V) dt)^{-1}$ is not necessarily diagonal any more, though.

3.3 Accuracy of the reduction approaches

A global error analysis is difficult due to the nonlinearity of (OED). We start by looking at the objective function ϕ for fixed controls u and sampling decisions w . Obviously, the values of $\phi(F_l(t_f))$ and of

$$\phi(F_l(t_f)) = \phi \left(\begin{pmatrix} F_{\hat{p}\hat{p}} & F_{\hat{p}c}\Xi_l \\ \Xi_l^T F_{\hat{p}c}^T & \Xi_l^T F_{cc}\Xi_l \end{pmatrix} \right)$$

depend heavily on the weights θ of the ANN. Even for the simpler case $n_{\hat{p}} = 0$ it is not clear how the scalar $\phi(\Xi_l^T F_{cc} \Xi_l) = \Xi_l^T F_{cc} \Xi_l$ and the value $\phi(F_{cc})$ are related. The situation is clearer for the SVD approach. Here the decompositions $F(t_f) = F_{cc}(t_f) = \hat{V}\hat{D}\hat{V}^T = \sum_{i=1}^{n_{\theta}} \lambda_i v_i v_i^T$ and $F_{\text{SVD}_{n_s}}(t_f) = VDV^T = \sum_{i=1}^{n_s} \lambda_i v_i v_i^T$ with eigenvalues λ_i assumed to be positive can be used to derive

$$\phi_A(F(t_f)) - \phi_A(F_{\text{SVD}_{n_s}}(t_f)) = \frac{1}{n_{\theta}} \sum_{i=1}^{n_{\theta}} \frac{1}{\lambda_i} - \frac{1}{n_s} \sum_{i=1}^{n_s} \frac{1}{\lambda_i} \quad (24)$$

$$\phi_D(F(t_f)) - \phi_D(F_{\text{SVD}_{n_s}}(t_f)) = \prod_{i=1}^{n_{\theta}} \frac{1}{\lambda_i^{n_{\theta}}} - \prod_{i=1}^{n_s} \frac{1}{\lambda_i^{n_s}} \quad (25)$$

$$\phi_E(F(t_f)) - \phi_E(F_{\text{SVD}_{n_s}}(t_f)) = \max_{1 \leq i \leq n_{\theta}} \frac{1}{\lambda_i} - \max_{1 \leq i \leq n_s} \frac{1}{\lambda_i} = \frac{1}{\lambda_{n_{\theta}}} - \frac{1}{\lambda_{n_s}} \geq 0 \quad (26)$$

These estimations, however, are based on identical u^* and w^* , which is typically not the case due to the modification of the optimization problem. Already the question how $\phi(F_{\text{SVD}_{n_s}}(t_f))$ changes with w is nontrivial. Here, error bounds for the truncated singular value decomposition [88] or for eigenvalues of sums of Hermitian matrices as investigated by Knutson and Tao [48] might be an interesting line of research. We are also interested in the sensitivity of the resulting experiment as parameterized via u and w . Given the difficulty of this task, we focus on an analysis of changes in w that is based on local necessary conditions of optimality. This is facilitated by the fact that in the continuous formulation well-posed OED control problems have bang-bang solutions in w , i.e., we have $w_i^*(t) \in \{0, 1\}$ for t almost everywhere. In [77], application of Pontryagin's maximum principle to (OED) resulted in the concept of information gain.

Definition 5. (Local and global information gain)

The maps $P^i : \mathcal{T} \mapsto \mathbb{R}^{n_p \times n_p}$ for $i \in [n_y]$ defined with matrices

$$P^i(t) := (h_x^i(x(t))G(t))^T (h_x^i(x(t))G(t))$$

are called *local information gain*. Note that all $P^i(t)$ are positive semi-definite, and positive definite if the matrix $h_x^i(x(t))G(t)$ has full rank n_p .

If $F^{-1}(t_f)$ exists, we call the matrices $\Pi : \mathcal{T} \mapsto \mathbb{R}^{n_p \times n_p}$ defined by

$$\Pi^i(t) := F^{-1}(t_f)P^i(t)F^{-1}(t_f) \in \mathbb{R}^{n_p \times n_p}$$

the *global information gain* of measurement function i .

Lemma 6. (Minimize trace of covariance matrix) Let $\phi = \phi_A$ be the objective function of (OED), let $w^*(\cdot)$ be an optimal control function, and let μ^* be the vector of Lagrange multipliers of the constraints $z_i(t_f) \leq M_i$. If $w_i^*(t) = 1$, then

$$\text{trace}(\Pi^i(t)) \geq \mu_i^* n_p.$$

Lemma 7. (Minimize determinant of covariance matrix) *Let $\phi = \phi_D = (\det(F^{-1}(t_f)))^{\frac{1}{n_p}}$ be the objective function of (OED), let $w^*(\cdot)$ be an optimal control function, and let μ^* be the vector of Lagrange multipliers of the constraints $z_i(t_f) \leq M_i$. If $w_i^*(t) = 1$, then*

$$(\det(F^{-1}(t_f)))^{\frac{1}{n_p}} \sum_{i,j=1}^{n_p} (F(t_f))_{ij} (\Pi(t))_{ij} \geq \mu_i^* n_p.$$

The proofs follow from $\frac{\partial \text{trace}(A)}{\partial A} \Delta A = \text{trace}(\Delta A)$ and $\frac{\partial \det(A)}{\partial A} \Delta A = \det(A) \sum_{i,j=1}^{n_p} A_{ij}^{-1} \Delta A_{ij}$ for symmetric, positive definite matrices $A \in \mathbb{R}^{n \times n}$ and from analysis of Pontryagin’s maximum principle for the particular structures of (OED), see [77] for details and a similar result for ϕ_E .

These results allow to use the global information gains for an analysis of changes in w^* for different approximations of sensitivities. Comparing local sensitivity of optimal samplings w_i^* for, say, (OED-NN-1) and (OED-NN-SVD) hence boils down to a comparison of Lagrange multipliers and of the global information gains

$$\Pi_l^i(t) := F_l^{-1}(t_f) (h_x^i(x(t)) G_l(t))^T h_x^i(x(t)) G_l(t) F_l^{-1}(t_f) \quad (27)$$

and

$$\Pi_{\text{SVD}_{n_s}}^i(t) := F_{\text{SVD}_{n_s}}^{-1}(t_f) (h_x^i(x(t)) G_{\text{SVD}_{n_s}}(t))^T h_x^i(x(t)) G_{\text{SVD}_{n_s}}(t) F_{\text{SVD}_{n_s}}^{-1}(t_f) \quad (28)$$

As described in the literature, e.g., in [3], and plausible from the equations (24-26), the objective function ϕ_E is determined only by the smallest singular value λ_{n_s} , while the trace ϕ_A as the sum of the inverse singular values is dominated by several of the smallest eigenvalues, and the determinant ϕ_D is sensitive to the larger singular values. Given the specific situation of overparameterized ANN weights, this encourages the use of ϕ_D rather than ϕ_A or ϕ_E . When we compare the differences

$$\left| \det \Pi^i(t)^{\frac{1}{n_\theta}} - \det \Pi_{\text{SVD}_{n_s}}^i(t)^{\frac{1}{n_s}} \right| \quad (29)$$

and

$$\left| \frac{1}{n_\theta} \text{trace } \Pi^i(t) - \frac{1}{n_s} \text{trace } \Pi_{\text{SVD}_{n_s}}^i(t) \right| \quad (30)$$

a similar picture emerges. Multiplication with diagonal matrices with the inverses of λ_i on the main diagonal from left and from the right leads higher exponents λ_i^2 , but the different effect of multiplication for ϕ_D and for summation for ϕ_A is the same. While a detailed analytical study in full generality seems not to be very promising, the functions $\Pi_l^i(t)$ and $\Pi_{\text{SVD}_{n_s}}^i(t)$ and the dual variables μ can be useful for numerical insight and for heuristics. For example, application of the L-curve truncation criterion makes much sense also for the ϕ_A OED criterion and the UDE setting, because this is likely to result in more similar global information gain for (OED-NN-SVD $_{n_s}$) and (OED-NN-SVD $_{n_s+1}$). One line of future research beyond the scope of this paper is the question, how often and when during an optimization new SVD should be calculated, given that the SVD accuracy depends on the current optimization iterate. A comparison of (28) for different values of n_s might be a promising heuristic for this purpose. Another line of future work is that the information gain functions might be used for penalizations of overfitted ANNs in online OED for UDE, resulting in weights θ that perform similarly well in the training, but are regularized in a way such that an optimal sampling design is closer to that of more accurate but computationally more expensive approaches.

4 Numerical results

We provide implementation details of the novel methods and study illustrative UDE benchmark problems.

4.1 Implementation

Our code is implemented in `Julia` [8]. It uses the packages `Lux` [65] for modeling, training, and evaluation of ANN and `DynamicOED.jl` [59] for setting up the OED problems, e.g., augmenting the user-defined dynamical system by VDE for the sensitivities G and the differential equations to evaluate the FIM $F(t_f)$, its inverse, and objective functions ϕ . Several approaches for reducing computational effort have been implemented. For example, for fixed controls u and initial values x_0 , i.e. for OED problems where only the sampling decisions w remain as degrees of freedom for the optimization, the states x and the sensitivities G are only computed once. The sampling decisions $w(t) \in \Omega = \{0, 1\}^{n_y}$ can be relaxed to $w(t) \in \text{conv } \Omega = [0, 1]^{n_y}$, allowing for an efficient solution via local nonlinear programming solvers such as `Ipopt` [89]. A theoretical justification for the relaxation was given in [77]. Optimal solutions for relaxed sampling decisions on well-chosen time discretization grids typically already fulfill integrality due to a bang-bang property of w .

The implemented sequential procedure that mimicks application of OED to obtain data from real experiments is identical and can be summarized as follows.

Algorithm 1. (General sequential evaluation procedure)

1. Fix \hat{p} . Create synthetical data based on $\bar{f}(x, \hat{p})$ and train $U(x, \theta)$ to obtain an initial guess $\bar{\theta}$
2. Solve (OED) for $\bar{p} = (\hat{p}, \bar{\theta})$ and obtain optimal controls and samplings (u^*, w^*)
3. Create synthetical data based on the values of $w_i^*(t) \in [0, 1]$ and on the observation functions $h^i(x^*(t))$
4. Solve a combined parameter estimation and ANN training problem to obtain updated values for (\hat{p}, θ)
5. Evaluate performance criterium

In step 1., weights θ may already be available as the result of an initial training on existing data, or synthetic data based on prior guesses on the dynamics. In this study, we generate synthetic data and perform an initial training to obtain a function $U(x, \theta)$ such that the initial value problem (2) has a unique solution.

In some scenarios, the degrees of freedom in 2. are restricted, e.g., to compare results for the cases where the control u is fixed or the sampling is equidistant and not a degree of freedom.

In step 3. of Algorithm 1, we evaluate $h^i(x^*(t_j))$ at times t_j that are determined as follows. In the direct approach we use to solve (OED), $w(t)$ is discretized as $w_{i,j} \in [0, 1]$ for $i \in [n_y]$ and $j \in [N]$ with $N \in \mathbb{N}$ being the number of discretization intervals. We normalize the optimal discretized solution $w_{i,j}^*$ by dividing by the corresponding bound M_i on the measurements for each measurement function h^i , i.e., $\bar{w}_{i,j}^* = w_{i,j}^*/M_i$, $i \in [n_y]$, $j \in [N]$ and interpret the elements of \bar{w}^* as probabilities. For each measurement function we then sample the wanted number of measurement time points without replacement. A discrete measurement time point for measurement function h^i is added at $\frac{t_{j-1} + t_j}{2}$ if $w_{i,j}$ was selected, where t_{i-1} and t_i are the start and end points of the i -th discretization interval, for $i \in [N]$. The values $h^i(x^*(t_j))$ are then modified with normally distributed noise.

Concerning step 4., efficient algorithms for the concurrent estimation of model parameters and weights are an open research topic. For the small-scale illustrative hybrid benchmark examples in this paper, we apply an iterative heuristic procedure: we use the two different approaches alternatingly by fixing either \hat{p} or θ to the most recent estimation, until the model parameters \hat{p} do not change any more. This allows to use standard approaches for the estimation of \hat{p} and the training of θ , respectively. For all parameter estimation problems we have been using a standard Gauß-Newton algorithm, for the training of the ANN we used the `Adam` algorithm [46]. To compensate the stochastic nature of ANN training, we averaged over five training runs from the same initial θ .

In step 5., the performance of a particular OED approach on the outcome of a follow-up parameter estimation / model training problem is evaluated. We did this using different approaches: a) by comparing parameter values and their uncertainty directly, b) by using the OED objective functions ϕ as an indicator for the uncertainty, c) based on simulations of the posterior distributions of the differential states x , and d) by comparing the absolute error between ANN $U(x, \theta)$ and the approximated ground-truth terms $\bar{f}(x, \hat{p})$ of the differential equation models over a domain of interest $x \in \mathcal{X}$.

4.2 Lotka-Volterra

The Lotka-Volterra equations are commonly used to describe population dynamics of interacting species, typically in a predator-prey relationship. We will use an extended version involving a fishing control u that was suggested to obtain a benchmark optimal control problem [78]. The ODE is given by

$$\begin{aligned}\dot{x}_1(t) &= x_1(t) - \hat{p}_1 x_1(t) x_2(t) - \hat{p}_2 u(t) x_1(t), \\ \dot{x}_2(t) &= -x_2(t) + \hat{p}_3 x_1(t) x_2(t) - \hat{p}_4 u(t) x_2(t), \\ x(0) &= x_0\end{aligned}\tag{31}$$

with a time horizon $\mathcal{T} = [0, 12]$, model parameters $\hat{p}_1 = 1.0$, $\hat{p}_2 = 0.4$, $\hat{p}_3 = 1.0$, $\hat{p}_4 = 0.2$, a control function $u(t) \in [0, 1]$ and fixed initial values $x_0 = (0.7, 0.5)$. We assume that we can directly measure the states separately via $h^1(x(t)) = x_1(t)$, $h^2(x(t)) = x_2(t)$ with a limit of $M_1 = M_2 = 3$ time units each.

To study hybrid modeling, we assume the interaction terms $x_1(t)x_2(t)$ to be unknown. We replace it in (31) with an ANN $U : \mathbb{R}^2 \times \mathbb{R}^{n_\theta} \mapsto \mathbb{R}$ and obtain

$$\begin{aligned}\dot{x}_1(t) &= x_1(t) - U(x(t), \theta) - \hat{p}_2 u(t) x_1(t), \\ \dot{x}_2(t) &= -x_2(t) + U(x(t), \theta) - \hat{p}_4 u(t) x_2(t), \\ x(0) &= x_0\end{aligned}\tag{32}$$

The ANN U has two hidden layers with ten neurons each, using the *tanh* activation function $\tanh(x) = \frac{\exp(x) - \exp(-x)}{\exp(x) + \exp(-x)}$ in all hidden layers. The output layer is equipped with the *softplus* function $\text{softplus}(x) = \ln(1 + \exp(x))$. This way, the a-priori knowledge that the correct term in the right-hand side is positive at all times for positive initial values x_0 can be easily incorporated. The total amount of weights and biases of this net is $n_\theta = 151$.

In the following subsections we study OED problems based on (31-32) with different combinations of model parameters \hat{p} and weights θ by application of Algorithm 1.

4.2.1 Estimating mechanistic model parameters

We start by considering OED for the ODE (31). As in [77], we assume the model parameters \hat{p}_2 and \hat{p}_4 to be known and calculate experiments that provide rich information for estimating the model parameters (\hat{p}_1, \hat{p}_3) . We consider four different OED problems in step 2. of Algorithm 1, combining a) equidistant and free sampling w with b) fixed controls $u \equiv 0$ and optimal controls $u \equiv u^*$. In all cases, in step 1. of Algorithm 1 we sample $\hat{p}_i \sim \mathcal{N}(1.0, 0.25^2)$, $i \in \{1, 3\}$, in step 3. we select three measurement times in \mathcal{T} per differential state, and in step 3. we add normally distributed noise with mean 0 and variance $\sigma^2 = 0.1^2$.

The results of the parameter estimation problems are given in Table 1.

Approach		\hat{p}_1	\hat{p}_3
$u \equiv 0$	w equidistant	0.998 ± 0.057	0.980 ± 0.082
	$w = w^*$	1.005 ± 0.037	1.008 ± 0.034
$u = u^*$	w equidistant	1.013 ± 0.055	1.003 ± 0.004
	$w = w^*$	0.995 ± 0.017	1.004 ± 0.006

Table 1: Comparison of parameter estimates and their uncertainty for the four considered OED problems varying in constraints on u and w .

While three equidistant measurements suffice to determine the two parameters with a maximum error of 2%, a significant improvement in accuracy and in the reduction of uncertainty can be observed when timing the measurements optimally or stimulating the system with controls u^* . The effect is even stronger when both are combined. The more accurate and less uncertain parameter estimates directly carry over to more accurate predictions in the differential states and the interaction terms, as shown in Figure 3.

Figure 4 illustrates Lemma 6 and the concept of global information gain.

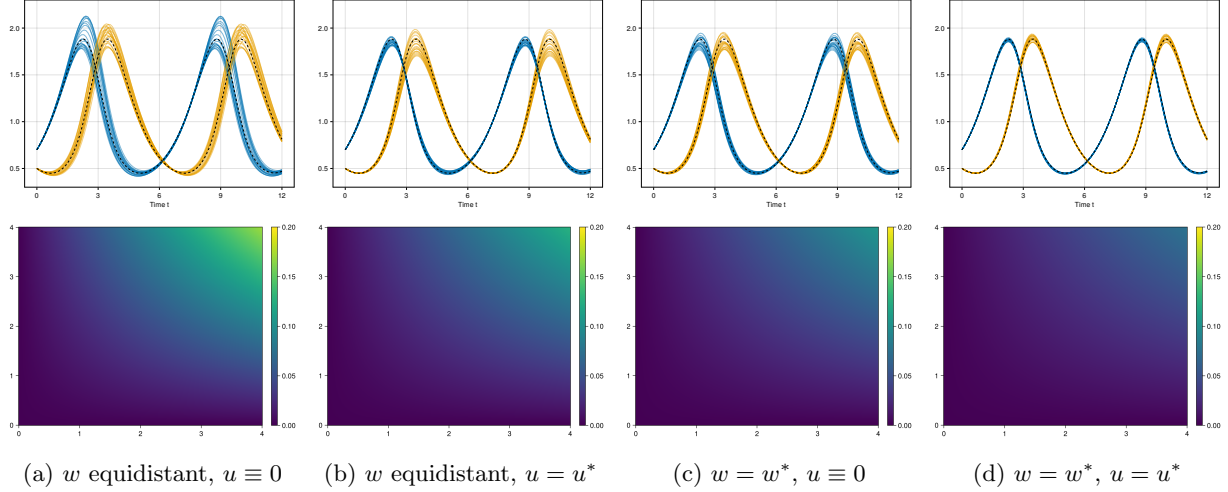


Figure 3: Top row: Monte-Carlo simulations of (31) using the parameter estimates and uncertainties from Table 1. Bottom row: absolute errors of interaction term $|\hat{p}_i \cdot x_1 x_2 - x_1 x_2|$ averaged for $i = 1, 3$ on $\mathcal{X} = [0, 4]^2$. Both rows (from left to right) show that solving (OED) reduces the uncertainty significantly.

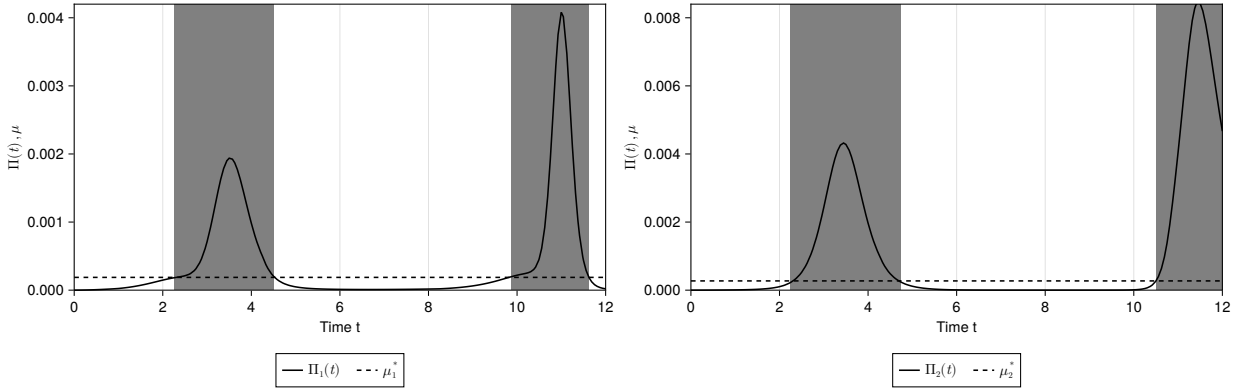


Figure 4: The Lagrange multipliers μ^* of the constraints $z_i(t_f) \leq M_1$ and the function $\text{trace}(\Pi^i(t))$ are plotted for the two measurement functions $h^i(x(t)) = x_i(t)$ together with optimal sampling functions $w_i^*(\cdot)$. As stated in Lemma 6, if $w_i^*(t) = 1$, then $\text{trace}(\Pi^i(t)) \geq \mu_i^* n_p$.

4.2.2 Training of ANN weights

Now we consider the UDE (32) for OED problems that differ in constraints on (u, w) in step 2. of Algorithm 1 as in Section 4.2.1, but also in the chosen approach (OED-NN-I), (OED-NN-II), and (OED-NN-SVD $_{n_s}$) for various numbers n_s of singular values to approximate the FIM of the overparameterized ANN training problem. We use a similar procedure as in Section 4.2.1, but increase the maximum number of measurements per differential state in step 3. to ten. A prototypical solution of problem (OED) is shown in Figure 5. As expected, the resulting optimal controls and states are qualitatively similar to those for the mechanistic ODE considered in Section 4.2.1 and in [77]. The control excites the differential states towards higher oscillations which go along with increased oscillations also in the sensitivities. This way, more information can be collected in regions of the state-space where the model is highly sensitive towards the weights and biases θ .

Looking in more detail into differences of the various approaches, we can observe a decrease in uncertainty measured in the objective function $\phi_{\text{SVD}_{n_s}}$ if OED is applied, see Table 2. The deviation of weights θ^* from the initial weights $\bar{\theta}$ is not a reliable indicator, though, because of the overparameterized ANN, and only shown for completeness. There are two trends observable in the table. First, taking measure-

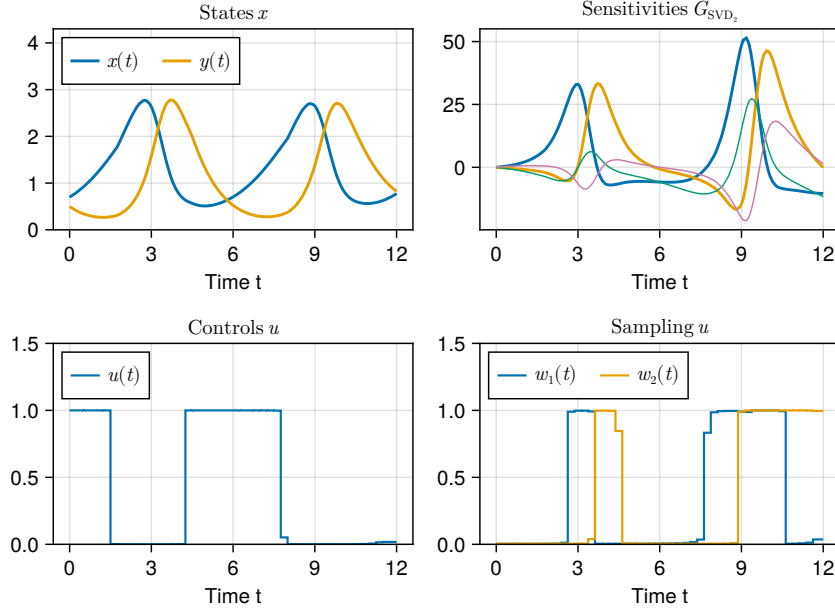


Figure 5: Solution of (OED) for (32) with the embedded ANN using the (OED-NN-SVD₂) approach.

Approach		$\phi_{\text{SVD}_{n_s}}(w, u)$	$ \Delta\theta _2$	Approach		$\phi_{\text{SVD}_{n_s}}(w, u)$	$ \Delta\theta _2$
$u \equiv 0$	Equidistant	5.25e-3	0.25	$u = u^*$	Equidistant	7.12e-4	1.91
	OED-NN-I	2.34e-3	0.73		OED-NN-I	1.59e-4	2.31
	OED-NN-II	2.40e-3	0.32		OED-NN-II	1.63e-4	1.85
	OED-SVD ₂	2.33e-3	0.33		OED-SVD ₂	1.53e-4	2.51

Table 2: D-Criterion ϕ_D of the SVD-based OED approach and averaged deviation of trained weights θ^* from the initial weights $\bar{\theta}$. Compared are the OED problems corresponding to fixed and free controls u , and for different dimension reduction approaches, respectively.

ments at optimized time points compared to equidistant measurements yields a noticeable reduction in the objective, regardless whether controls are optimized along with the sampling decision or not. Second, applying optimized controls $u^*(t)$ reduces the objective for almost all strategies by approximately one order of magnitude.

Another evaluation criterium is the comparison of absolute errors of ground truth model and ANN output $U(x, \theta^*)$ over a domain of interest \mathcal{X} . Figure 6 shows the increase in accuracy due to OED. One observes advantages for the SVD approach, and in general for all OED problems with additional degrees of freedom. Of particular interest is the correspondence between OED solutions with optimal u^* resulting in a larger training domain (see also Figure 5 for the increased oscillations of x), and the increased accuracy for the extrapolated domain $\mathcal{X} = [0, 4]^2$ (as compared to the originally considered state-space domain $\mathcal{X} = [0, 2]^2$). We observe improvements in the average accuracy between 33% and 56%.

Finally, we have a look at the global information gain function also for our reduced OED approaches.

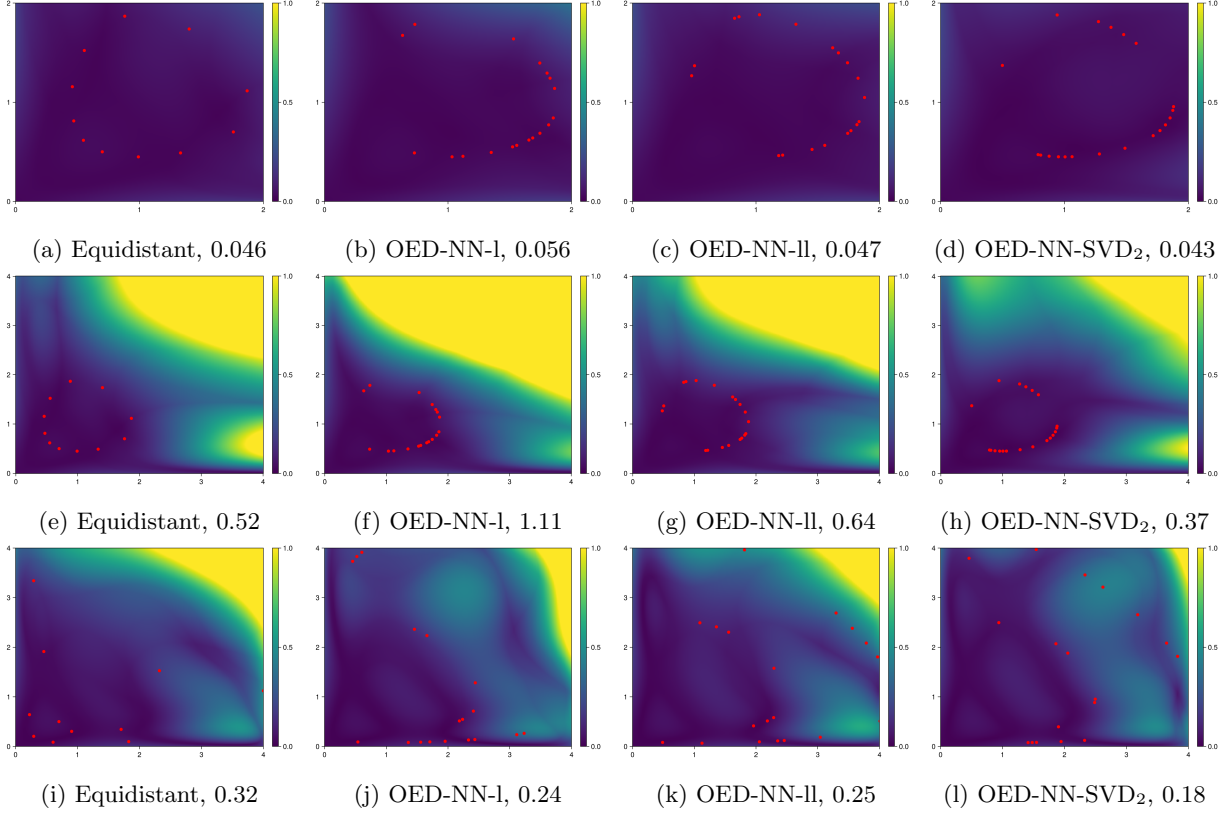


Figure 6: Absolute errors of trained neural networks $|U(x, y) - x \cdot y|$ each averaged over five training runs started from initial θ . The captions denote the applied strategy and the average absolute error. Dotted in red are 10 measurements per differential state which have been chosen according to the calculated optimal experimental design. First row: Errors on domain $[0, 2]^2$ for OED with fixed $u(t) = 0$. Second row: The same weights as in the first row, but now evaluated on $[0, 4]^2$. Third row: as above, but with $u(t) = u^*(t)$. While in this case improvements due to sampling are not significant and might be dominated by training noise (first two rows), additional excitation of the system (third row) leads to clearly increased accuracy.

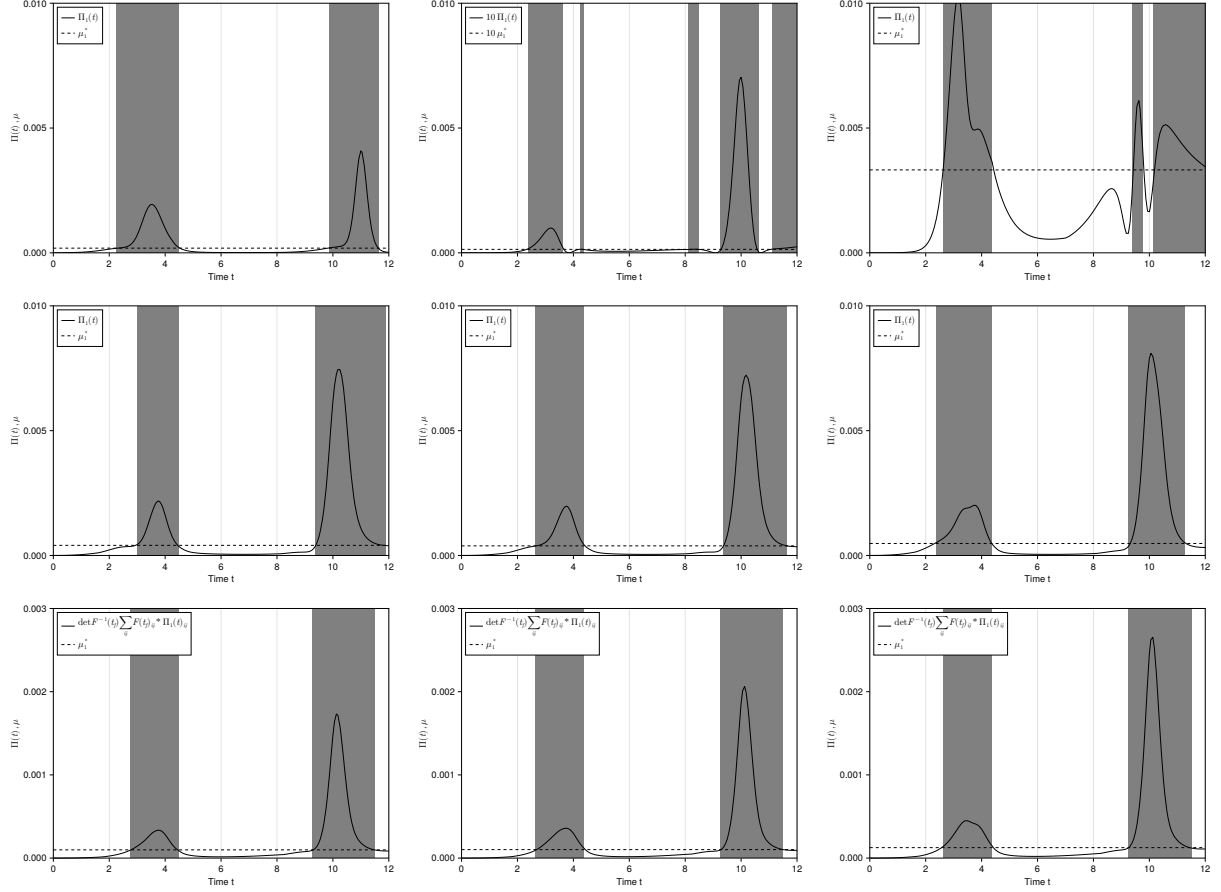


Figure 7: Comparison of global information gain functions for the case $(w, u) = (w^*, u^*)$ applied to the first observation function $h^1(x(t))$ of the Lotka Volterra OED problem. The time intervals in which the optimal samplings w^* take the value 1 are indicated in grey. As postulated in Lemmata 6 and 7 from Section 3.3, they correspond to times t when functions of the global information gain exceed the Lagrange multiplier μ . While the optimal samplings w^* for the lumped approaches (top row middle and right) differ from the optimal sampling of the pure ODE approach from Section 4.2.1 (top left), one sees a clear convergence of the SVD samplings for larger values of $n_s = 7, 8, 9$ (middle row). This effect is even stronger in case of the ϕ_D criterion (bottom row).

4.2.3 Concurrent training of ANN weights and estimation of model parameters

We now consider the situation where both model parameters \hat{p} and ANN weights θ shall be updated from experimental data. We consider the case in which the parameter \hat{p}_2 is uncertain in addition to the weights of the ANN $U(x, \theta)$ studied in the previous section. Table 3 shows the objective function values of the different OED approaches.

	Approach	$\phi_{\text{SVD}_{10}}(w, u)$
$u = u^*$	Equidistant	9.49e-2
	OED-NN-1	3.91e-2
	OED-NN-11	9.65e-2
	OED-NN-SVD ₁	3.80e-2
	OED-NN-SVD ₂	3.40e-2
	OED-NN-SVD ₃	4.49e-2
	OED-NN-SVD ₄	3.56e-2
	OED-NN-SVD ₅	3.86e-2
	OED-NN-SVD ₆	3.64e-2
	OED-NN-SVD ₇	3.17e-2
	OED-NN-SVD ₈	3.03e-2
	OED-NN-SVD ₉	3.02e-2
	OED-NN-SVD ₁₀	3.00e-2

Table 3: A-Criterion ϕ_A of the SVD₁₀-based OED approach. The uncertainty as measured via ϕ is reduced with increasing number of singular values. Lumping of parameters performs almost similarly well when compared to OED-NN-SVD _{n_s} approaches.

In Figure 8 some corresponding sensitivities are plotted, illustrating the relation between lumping and singular value decomposition.

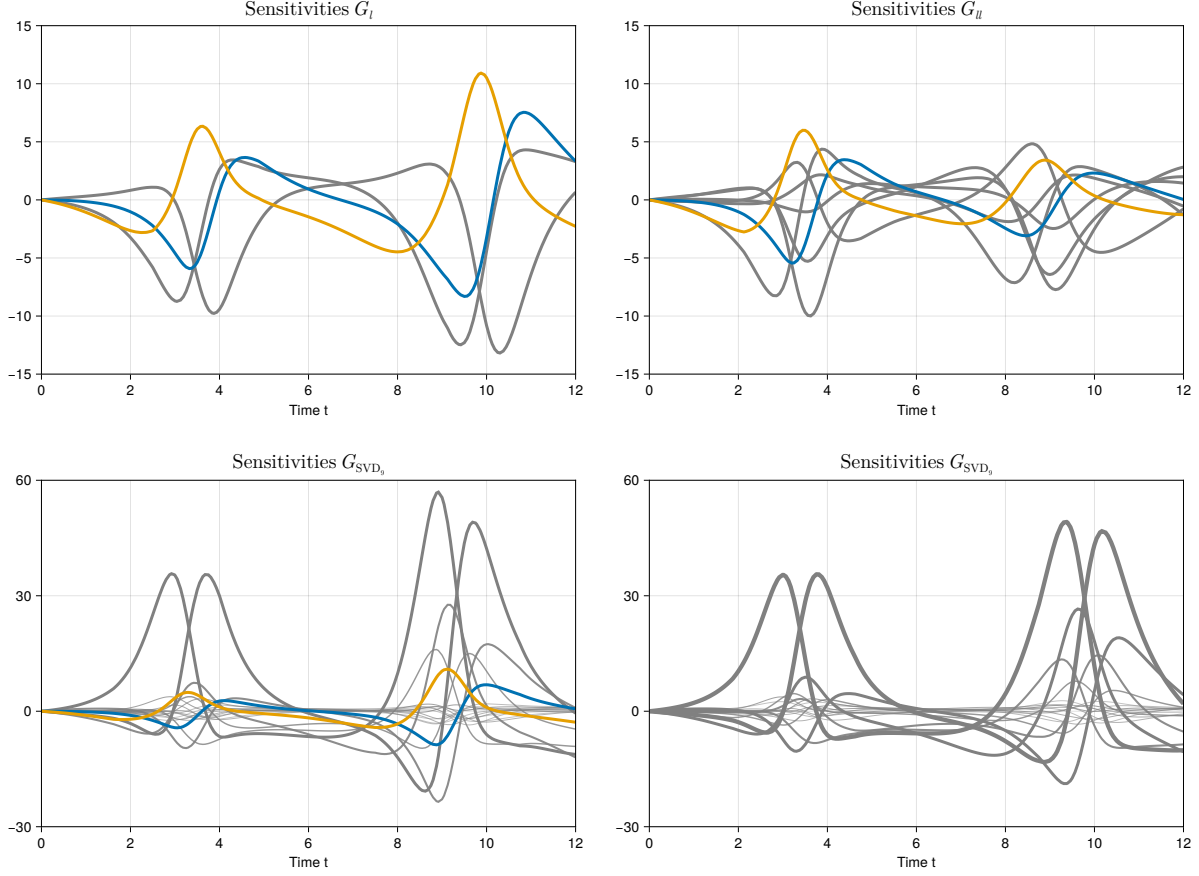


Figure 8: Comparison of sensitivities for different dimension reduction approaches applied to OED for concurrent training of ANN weights and model parameters of the Lotka-Volterra UDE. The line width of trajectories indicates the size of the corresponding singular values. While the lumped and layerwise-lumped approach are shown in the top row, the bottom row shows trajectories for the case where \hat{p}_2 is independent (left, sensitivities corresponding to \hat{p}_2 shown in color) or integrated in the SVD approach.

4.3 Urethane reaction

We consider the chemical reaction of urethane investigated in [49, 51]. The reaction is given by the scheme



with educts isocyanate A , butanol B , value product urethane C , downstream product allophanate D , by-product isocyanurate E and solvent dimethylsulfoxide L . It can be described by the system of ODEs

$$\begin{aligned} \dot{n}_C &= V \cdot (r_1 - r_2 + r_3) \\ \dot{n}_D &= V \cdot (r_2 - r_3) \\ \dot{n}_E &= V \cdot (r_4) \\ \dot{n}_A &= V \cdot (-r_1 - r_2 + r_3 - 3r_4) + u_1(t) \\ \dot{n}_B &= V \cdot (-r_1) + u_2(t) \\ \dot{n}_L &= u_1(t) + u_2(t), \\ \dot{T}(t) &= u_T(t). \end{aligned} \tag{34}$$

The reaction rates r_i are given by $r_1 = k_1 \frac{n_A}{V} \frac{n_B}{V}$, $r_2 = k_1 \frac{n_A}{V} \frac{n_C}{V}$, $r_3 = k_3 \frac{n_D}{V}$, and $r_4 = k_4 \left(\frac{n_L}{V}\right)^2$, respectively, using the reaction volume

$$V = \frac{n_A \cdot M_A}{\rho_A} + \frac{n_B \cdot M_B}{\rho_B} + \frac{n_C \cdot M_C}{\rho_C} + \frac{n_D \cdot M_D}{\rho_D} + \frac{n_E \cdot M_E}{\rho_E} + \frac{n_L \cdot M_L}{\rho_L},$$

and Arrhenius equations for the dependency of the reaction rate on the temperature T

$$\begin{aligned} k_1 &= k_{ref1} \cdot \exp\left(-\frac{E_{a1}}{R} \cdot \left(\frac{1}{T} - \frac{1}{T_{ref}}\right)\right), \\ k_2 &= k_{ref2} \cdot \exp\left(-\frac{E_{a2}}{R} \cdot \left(\frac{1}{T} - \frac{1}{T_{ref}}\right)\right), \\ k_4 &= k_{ref4} \cdot \exp\left(-\frac{E_{a4}}{R} \cdot \left(\frac{1}{T} - \frac{1}{T_{ref}}\right)\right), \\ k_C &= k_{C2} \cdot \exp\left(-\frac{\Delta H_2}{R} \cdot \left(\frac{1}{T} - \frac{1}{T_{ref}}\right)\right), \\ k_3 &= \frac{k_2}{k_c} \end{aligned}$$

with steric factors $k_{ref1}, k_{ref2}, k_{ref4}$, activation energies E_{a1}, E_{a2}, E_{a4} , equilibrium constant K_{C2} , reaction enthalpy ΔH_2 , and reference reaction temperature T_{ref} as parameters. The initial values of the products are set to zero, i.e.,

$$n_C(t_0) = n_D(t_0) = n_E(t_0) = 0.$$

Time-independent control values are given by the initial values of the educts

$$n_A(t_0) = n_{A0}, n_B(t_0) = n_{B0}, n_L(t_0) = n_{L0}.$$

Furthermore, the control functions $u_1(t), u_2(t), u_T(t)$, $t \in [t_0, t_f]$ influence the evolution of the two feeds and the temperature $T(t)$, respectively.

We assume that the reaction rate for the reaction of isocyanate to isocyanurate is unknown and needs to be learned from experimental data and thus replace r_4 by an ANN. We thereby obtain a hybrid ODE model

$$\begin{aligned}
\dot{n}_C &= V \cdot (r_1 - r_2 + r_3) \\
\dot{n}_D &= V \cdot (r_2 - r_3) \\
\dot{n}_E &= V \cdot (U((n_C, n_D, n_E, n_A, n_B, n_L), \theta)) \\
\dot{n}_A &= V \cdot (-r_1 - r_2 + r_3 - 3U((n_C, n_D, n_E, n_A, n_B, n_L), \theta)) + u_1(t) \\
\dot{n}_B &= V \cdot (-r_1) + u_2(t) \\
\dot{n}_L &= u_1(t) + u_2(t), \\
\dot{T}(t) &= u_T(t).
\end{aligned} \tag{35}$$

Moreover, we assume that the steric factor k_{ref_1} and the activation energy E_{a1} are uncertain parameters \hat{p} . Hence, we solve the problem (OED) for the concurrent estimation of parameters k_{ref_1} and E_{a1} and the weights θ . For illustration purposes we restrict ourselves to the calculation of optimal feeds $u_1(t), u_2(t)$ with fixed initial values $n_{A0} = 0.1$ mol, $n_{B0} = 0.05$ mol, $n_{L0} = 0.0$ mol, and fixed temperature profile given by a linear increase from $T(0h) = 300K$ to $T(80h) = 400K$.

Table 4 shows the OED objective function values for different approaches. Again, lumping all weights performs better than layerwise lumping, however somewhat worse than the SVD approaches. The non-monotonicity with respect to increasing numbers of singular values indicated the effect of noise on the results, though.

Approach		$\phi_{\text{SVD}_{n_s}}(w, u)$
$u = u^*$	Equidistant	1-05e-2
	OED-NN-I	7.23e-3
	OED-NN-II	2.46e-2
	OED-NN-SVD ₁	2.00e-2
	OED-NN-SVD ₂	4.76e-3
	OED-NN-SVD ₃	1.12e-3
	OED-NN-SVD ₄	1.12e-3
	OED-NN-SVD ₅	2.16e-3

Table 4: A-Criterion of the SVD-based OED approach. Compared are the OED problems corresponding to fixed and free controls u , and for different dimension reduction approaches, respectively.

Again, we study the corresponding sensitivities in Figure 9.

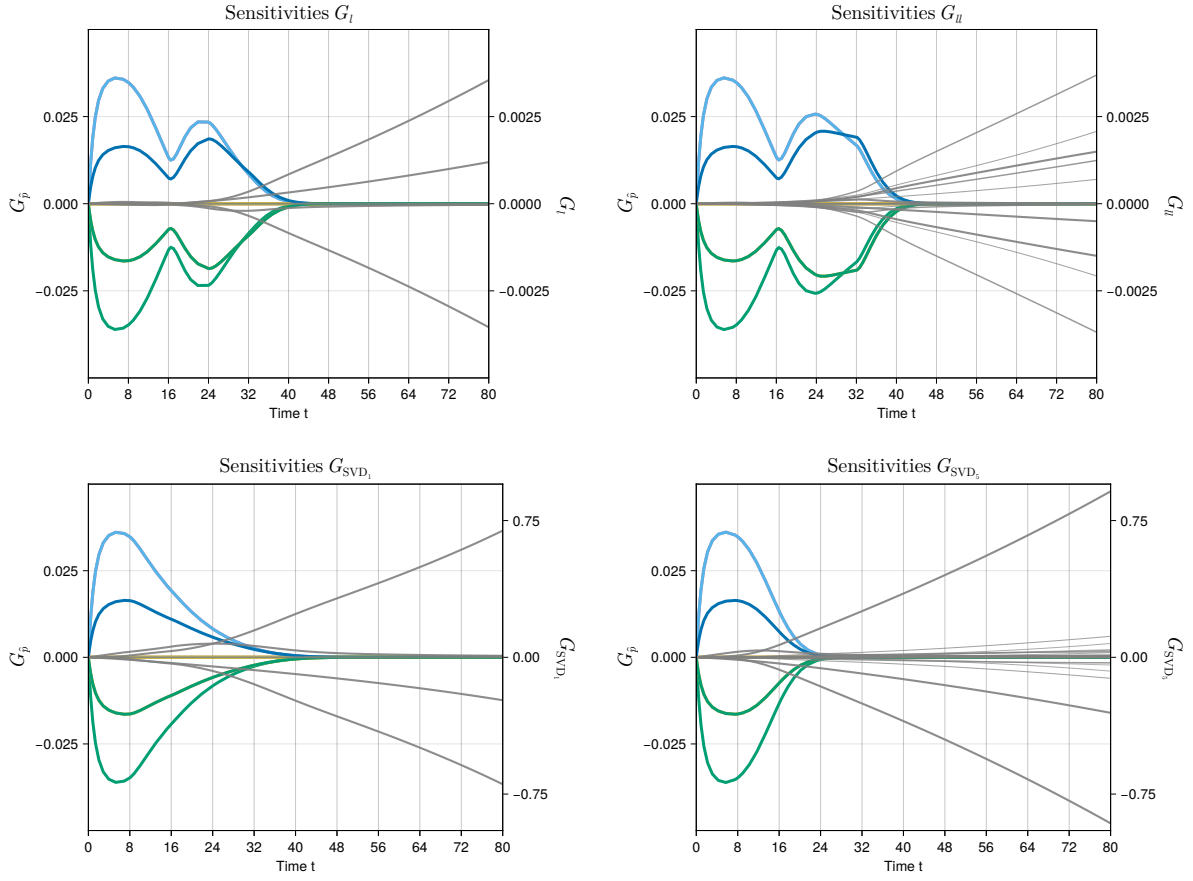


Figure 9: Visualization of the sensitivities G_I , G_{II} , G_{SVD_1} , and G_{SVD_5} . Sensitivities for the model parameters \hat{p} are highlighted in color.

5 Discussion and outlook

We discussed optimum experimental design for universal differential equations. In particular, we compared a novel sensitivity lumping approach as an alternative to the established truncated SVD method. It uses the trick of an artificial scaling parameter with value 1.0 to derive a simple multiplication formula for the dimension reduction of the sensitivity equations that uses the current ANN weight estimate.

By implementing all algorithms based on the julia package `DynamicOED.jl` we created a modular platform that allows to solve challenging OED problems and compare novel algorithmic ideas. Active learning for hybrid problems can thus be treated by efficient numerical algorithms for optimal control.

Part of this comparison is the analysis of global information gain, which yields necessary conditions of optimality for the sampling decisions w . We motivated that this could be used in the future as a criterion for deciding the truncation point of SVD, for determining when to update SVD decompositions during an optimization algorithm, or to derive penalizations for the training of ANN weights resulting in better sampling decisions.

In summary, lumping approaches might become a feasible alternative to established reduction approaches for OED of UDE problems, especially when singular value decompositions become computationally expensive due to the size of the involved ANN.

Acknowledgements This project has received funding from the European Regional Development Fund (grants `timingMatters` and `IntelAlgen`) under the European Union’s Horizon Europe Research and Innovation Program, from the German Research Foundation DFG within GRK 2297 ‘Mathematical Complexity Reduction’ and priority program 2331 ‘Machine Learning in Chemical Engineering’ under grants KI 417/9-1, SA 2016/3-1, SE 586/25-1, which we gratefully acknowledge.

References

- [1] A.C. Atkinson and A. Donev. *Optimum Experimental Designs*. Number 8 in Oxford Statistical Sciences Series. Oxford University Press, Oxford, 1992.
- [2] Vernon Austel, Sanjeeb Dash, Oktay Gunluk, Lior Horesh, Leo Liberti, Giacomo Nannicini, and Baruch Schieber. Globally optimal symbolic regression. *arXiv preprint arXiv:1710.10720*, October 2017.
- [3] Tilman Barz, Stefan Körkel, Günter Wozny, et al. Nonlinear ill-posed problem analysis in model-based parameter estimation and experimental design. *Computers & Chemical Engineering*, 77:24–42, 2015.
- [4] Tilman Barz, Diana C López Cárdenas, Harvey Arellano-Garcia, and Günter Wozny. Experimental evaluation of an approach to online redesign of experiments for parameter determination. *AIChE Journal*, 59(6):1981–1995, 2013.
- [5] P. Benner, S. Grivet-Talocia, A. Quarteroni, G. Rozza, W. H. A. Schilders, and L. M. Silveira, editors. *Model Order Reduction. Volume 1: System- and Data-Driven Methods and Algorithms / Volume 2: Snapshot-Based Methods and Algorithms / Volume 3: Applications*. De Gruyter, Berlin, 2021.
- [6] P. Benner, S. Gugercin, and K. Willcox. A survey of projection-based model reduction methods for parametric dynamical systems. *SIAM Review*, 57(4):483–531, 2015.
- [7] Dimitris Bertsimas and Wes Gurnee. Learning sparse nonlinear dynamics via mixed-integer optimization. *Nonlinear Dyn.*, 111(7):6585–6604, January 2023.
- [8] Jeff Bezanson, Alan Edelman, Stefan Karpinski, and Viral B Shah. Julia: A fresh approach to numerical computing. *SIAM review*, 59(1):65–98, 2017.
- [9] L.T. Biegler. *Nonlinear Programming: Concepts, Algorithms, and Applications to Chemical Processes*. Series on Optimization. SIAM, 2010.
- [10] Jordi Bolibar, Facundo Sapienza, Fabien Maussion, Redouane Lguensat, Bert Wouters, and Fernando Pérez. Universal differential equations for glacier ice flow modelling. *Geoscientific Model Development*, 16(22):6671–6687, November 2023.
- [11] Steven L Brunton and J Nathan Kutz. *Data-Driven Science and Engineering: Machine Learning, Dynamical Systems, and Control*. Cambridge University Press, 2022.
- [12] Steven L. Brunton, Joshua L. Proctor, and J. Nathan Kutz. Discovering governing equations from data by sparse identification of nonlinear dynamical systems. 113(15):3932–3937, 2016.
- [13] Martin Bubel, Jochen Schmid, Volodymyr Kozachynskyi, Erik Esche, and Michael Bortz. Sequential optimal experimental design for vapor-liquid equilibrium modeling. *arXiv preprint arXiv:2403.09443*, 2024.
- [14] Gustau Camps-Valls, Andreas Gerhardus, Urmi Ninad, Gherardo Varando, Georg Martius, Emili Balaguer-Ballester, Ricardo Vinuesa, Emiliano Diaz, Laure Zanna, and Jakob Runge. Discovering causal relations and equations from data. *Physics Reports*, 1044:1–68, 2023.
- [15] Ricky T. Q. Chen, Yulia Rubanova, Jesse Bettencourt, and David K Duvenaud. Neural Ordinary Differential Equations. In *Advances in Neural Information Processing Systems*, volume 31. Curran Associates, Inc., 2018.
- [16] David Cohn, Les Atlas, and Richard Ladner. Improving generalization with active learning. *Machine learning*, 15:201–221, 1994.
- [17] David A. Cohn. Neural Network Exploration Using Optimal Experiment Design. *Neural Networks*, 9(6):1071–1083, August 1996.
- [18] Alison Cozad and Nikolaos V Sahinidis. A global MINLP approach to symbolic regression. *Math. Program.*, 170(1):97–119, May 2018.

- [19] Karel Crombecq, Dirk Gorissen, Dirk Deschrijver, and Tom Dhaene. A novel hybrid sequential design strategy for global surrogate modeling of computer experiments. *SIAM Journal on Scientific Computing*, 33(4):1948–1974, 2011.
- [20] G. Cybenko. Approximation by superpositions of a sigmoidal function. *Mathematics of Control, Signals and Systems*, 2(4):303–314, December 1989.
- [21] Kalyanmoy Deb. Multi-objective optimisation using evolutionary algorithms: an introduction. In *Multi-objective evolutionary optimisation for product design and manufacturing*, pages 3–34. Springer, 2011.
- [22] Francesco Di Fiore, Michela Nardelli, and Laura Mainini. Active learning and bayesian optimization: a unified perspective to learn with a goal. *Archives of Computational Methods in Engineering*, pages 1–29, 2024.
- [23] M. Diehl, H.G. Bock, J.P. Schlöder, R. Findeisen, Z. Nagy, and F. Allgöwer. Real-time optimization and Nonlinear Model Predictive Control of Processes governed by differential-algebraic equations. *J. Proc. Contr.*, 12(4):577–585, 2002.
- [24] Emilien Dupont, Arnaud Doucet, and Yee Whye Teh. Augmented Neural ODEs, October 2019.
- [25] Saso Dzeroski and Ljupco Todorovski. Equation discovery for systems biology: finding the structure and dynamics of biological networks from time course data. *Curr. Opin. Biotechnol.*, 19(4):360–368, August 2008.
- [26] John Eason and Selen Cremaschi. Adaptive sequential sampling for surrogate model generation with artificial neural networks. *Computers & Chemical Engineering*, 68:220–232, September 2014.
- [27] Carl Eckart and Gale Young. The approximation of one matrix by another of lower rank. *Psychometrika*, 1(3):211–218, September 1936.
- [28] Ahmed ElGazzar and Marcel van Gerven. Universal Differential Equations as a Common Modeling Language for Neuroscience, March 2024.
- [29] Srinivas Eswar, Vishwas Rao, and Arvind K Saibaba. Bayesian d-optimal experimental designs via column subset selection: The power of reweighted sensors. *arXiv preprint arXiv:2402.16000*, 2024.
- [30] Antonella Falini. A review on the selection criteria for the truncated svd in data science applications. *Journal of Computational Mathematics and Data Science*, 5:100064, 2022.
- [31] Meng Fang, Yuan Li, and Trevor Cohn. Learning how to active learn: A deep reinforcement learning approach. *arXiv preprint arXiv:1708.02383*, 2017.
- [32] V.V. Fedorov. *Theory of optimal experiments*. Academic Press, New York and London, 1972.
- [33] Federico Galvanin, Massimiliano Barolo, and Fabrizio Bezzo. Online Model-Based Redesign of Experiments for Parameter Estimation in Dynamic Systems. *Ind. Eng. Chem. Res.*, 2009. Published online on March 26, 2009.
- [34] Maximilian Gelbrecht, Valerio Lucarini, Niklas Boers, and Jürgen Kurths. Analysis of a bistable climate toy model with physics-based machine learning methods. *The European Physical Journal Special Topics*, 230(14-15):3121–3131, October 2021.
- [35] Amin Ghadami and Bogdan I Epureanu. Data-driven prediction in dynamical systems: recent developments. *Philos. Trans. A Math. Phys. Eng. Sci.*, 380(2229):20210213, August 2022.
- [36] P. Goyal and P. Benner. Neural ordinary differential equations with irregular and noisy data. *Roy. Soc. Open Sci.*, 10(7):221475, 2023.
- [37] Pawan Goyal and Peter Benner. Generalized quadratic embeddings for nonlinear dynamics using deep learning. *Physica D: Nonlinear Phenomena*, 463:134158, 2024.

- [38] Stewart Greenhill, Santu Rana, Sunil Gupta, Pratibha Vellanki, and Svetha Venkatesh. Bayesian optimization for adaptive experimental design: A review. *IEEE access*, 8:13937–13948, 2020.
- [39] Eldad Haber and Lars Ruthotto. Stable architectures for deep neural networks. *Inverse Problems*, 34(1):014004, December 2017.
- [40] Marvin Höge, Andreas Scheidegger, Marco Baity-Jesi, Carlo Albert, and Fabrizio Fenicia. Improving hydrologic models for predictions and process understanding using neural ODEs. *Hydrology and Earth System Sciences*, 26(19):5085–5102, October 2022.
- [41] Roger A Horn and Charles R Johnson. *Matrix analysis*. Cambridge university press, 2012.
- [42] Kurt Hornik. Approximation capabilities of multilayer feedforward networks. *Neural Networks*, 4(2):251–257, January 1991.
- [43] F. Jost, S. Sager, and T.T.T. Le. A feedback optimal control algorithm with optimal measurement time points. *Processes*, 5(10):1–19, 2017.
- [44] Tobias Kamp, Johannes Ultsch, and Jonathan Brembeck. Closing the Sim-to-Real Gap with Physics-Enhanced Neural ODEs:. In *Proceedings of the 20th International Conference on Informatics in Control, Automation and Robotics*, pages 77–84, Rome, Italy, 2023. SCITEPRESS - Science and Technology Publications.
- [45] Jongeun Kim, Sven Leyffer, and Prasanna Balaprakash. Learning symbolic expressions: Mixed-Integer formulations, cuts, and heuristics. *INFORMS J. Comput.*, July 2023.
- [46] Diederik P. Kingma and Jimmy Ba. Adam: A method for stochastic optimization. *CoRR*, abs/1412.6980, 2014.
- [47] C.P. Kitsos. *Optimal Experimental Design for Non-Linear Models*. Springer, Heidelberg, 2013.
- [48] Allen Knutson and Terence Tao. Honeycombs and sums of hermitian matrices. *Notices Amer. Math. Soc*, 48(2), 2001.
- [49] S. Körkel. *Numerische Methoden für Optimale Versuchsplanungsprobleme bei nichtlinearen DAE-Modellen*. PhD thesis, Universität Heidelberg, Heidelberg, 2002.
- [50] S. Körkel, I. Bauer, H.G. Bock, and J.P. Schlöder. A Sequential Approach for Nonlinear Optimum Experimental Design in DAE Systems. In *Scientific Computing in Chemical Engineering II*, pages 338–345. Springer, 1999.
- [51] S. Körkel, E. Kostina, H.G. Bock, and J.P. Schlöder. Numerical Methods for Optimal Control Problems in Design of Robust Optimal Experiments for Nonlinear Dynamic Processes. *Optimization Methods and Software*, 19:327–338, 2004.
- [52] Karina Koval, Roland Herzog, and Robert Scheichl. Tractable optimal experimental design using transport maps. *arXiv preprint arXiv:2401.07971*, 2024.
- [53] Clemens Kreutz and Jens Timmer. Systems biology: experimental design. *The FEBS Journal*, 276:923–942, 2009.
- [54] Roberto Lemoine-Nava, S F Walter, S Körkel, and S Engell. Online optimal experimental design: Reduction of the number of variables. *11th IFAC Symposium on Dynamics and Control of Process Systems*, 2016. Trondheim, Norway, 6–8 June 2016.
- [55] Niall M. Mangan, Steven L. Brunton, Joshua L. Proctor, and J. Nathan Kutz. Inferring biological networks by sparse identification of nonlinear dynamics. *IEEE Transactions on Molecular, Biological, and Multi-Scale Communications*, 2(1):52–63, 2016.

- [56] James Martens and Roger Grosse. Optimizing neural networks with kronecker-factored approximate curvature. In *Proceedings of the 32nd International Conference on International Conference on Machine Learning - Volume 37*, ICML’15, page 2408–2417. JMLR.org, 2015.
- [57] Carl Julius Martensen, Niklas Korsbo, Vijay Ivanturi, and Sebastian Sager. Data-driven discovery of feedback mechanisms in acute myeloid leukaemia. *preprint*, 2024.
- [58] Carl Julius Martensen, Christoph Plate, Tobias Keßler, Christian Kunde, Lothar Kaps, Achim Kienle, Andreas Seidel-Morgenstern, and Sebastian Sager. Towards Machine Learning of Power-2-Methanol Processes. In Antonios C. Kokossis, Michael C. Georgiadis, and Efstratios Pistikopoulos, editors, *Computer Aided Chemical Engineering*, volume 52 of *33 European Symposium on Computer Aided Process Engineering*, pages 561–568. Elsevier, January 2023.
- [59] Carl Julius Martensen, Christoph Plate, and Sebastian Sager. Dynamicoed.jl: A julia package for solving optimum experimental design problems. *Journal of Open Source Software*, 9(98):6605, 2024.
- [60] Luca Mencarelli, Qi Chen, Alexandre Pagot, and Ignacio E Grossmann. A review on superstructure optimization approaches in process system engineering. *Computers & Chemical Engineering*, 136:106808, 2020.
- [61] John Metzcar, Catherine R Jutzeler, Paul Macklin, Alvaro Köhn-Luque, and Sarah C Brüningk. A review of mechanistic learning in mathematical oncology. *Frontiers in Immunology*, 15:1363144, 2024.
- [62] Ruth Misener and Lorenz Biegler. Formulating data-driven surrogate models for process optimization. *Computers & Chemical Engineering*, 179:108411, 2023.
- [63] Mario S Mommer, Andreas Sommer, Johannes P Schlöder, and H Georg Bock. A nonlinear preconditioner for optimum experimental design problems. *EURO Journal on Computational Optimization*, 3(2):131–146, 2015.
- [64] Simon Olofsson, Marc Peter Deisenroth, and Ruth Misener. Design of experiments for model discrimination using gaussian process surrogate models. In *Computer Aided Chemical Engineering*, volume 44, pages 847–852. Elsevier, 2018.
- [65] Avik Pal. Lux: Explicit Parameterization of Deep Neural Networks in Julia, April 2023.
- [66] Michael Prince. Does active learning work? a review of the research. *Journal of engineering education*, 93(3):223–231, 2004.
- [67] F. Pukelsheim. *Optimal design of experiments*. Wiley, New York, 1993.
- [68] Jun Qian, Madiha Nadri, Petru-Daniel Moroşan, and Pascal Dufour. Closed loop optimal experiment design for on-line parameter estimation. In *Control Conference (ECC), 2014 European*, pages 1813–1818. IEEE, 2014.
- [69] C. Rackauckas, Y. Ma, J. Martensen, C. Warner, K. Zubov, R. Supekar, D. Skinner, and A. Ramadhan. Universal differential equations for scientific machine learning, 2020. arXiv preprint arXiv:2001.04385.
- [70] M. Raissi, P. Perdikaris, and G.E. Karniadakis. Physics-informed neural networks: A deep learning framework for solving forward and inverse problems involving nonlinear partial differential equations. *Journal of Computational Physics*, 378:686–707, 2019.
- [71] Ali Ramadhan, John Marshall, Andre Souza, Xin Kai Lee, Ulyana Piterbarg, Adeline Hillier, Gregory LeClaire Wagner, Christopher Rackauckas, Chris Hill, Jean-Michel Campin, and Raffaele Ferrari. Capturing missing physics in climate model parameterizations using neural differential equations, March 2023.
- [72] Karsten HG Rätze, Wieland Kortuz, Sabine Kirschtowski, Michael Jokiel, Christof Hamel, and Kai Sundmacher. Optimal experimental design for the identification of a reaction kinetic model for the hydroaminomethylation of 1-decene in a thermomorphic multiphase system. *Chemical Engineering Journal*, 469:143713, 2023.

- [73] Pengzhen Ren, Yun Xiao, Xiaojun Chang, Po-Yao Huang, Zhihui Li, Brij B Gupta, Xiaojiang Chen, and Xin Wang. A survey of deep active learning. *ACM computing surveys (CSUR)*, 54(9):1–40, 2021.
- [74] Julia Reuter, Manoj Cendrollu, Fabien Evrard, Sanaz Mostaghim, and Berend van Wachem. Towards Improving Simulations of Flows around Spherical Particles Using Genetic Programming. In *2022 IEEE Congress on Evolutionary Computation (CEC)*, pages 1–8, 2022.
- [75] Adrian Rojas-Campos, Lukas Stelz, and Pascal Nieters. Learning COVID-19 Regional Transmission Using Universal Differential Equations in a SIR model, November 2023.
- [76] Domenec Ruiz-Balet and Enrique Zuazua. Neural ode control for classification, approximation, and transport. *SIAM Review*, 65(3):735–773, 2023.
- [77] S. Sager. Sampling Decisions in Optimum Experimental Design in the Light of Pontryagin’s Maximum Principle. *SIAM Journal on Control and Optimization*, 51(4):3181–3207, 2013.
- [78] S. Sager, H.G. Bock, M. Diehl, G. Reinelt, and J.P. Schlöder. Numerical methods for optimal control with binary control functions applied to a Lotka-Volterra type fishing problem. In A. Seeger, editor, *Recent Advances in Optimization*, volume 563 of *Lectures Notes in Economics and Mathematical Systems*, pages 269–289, Heidelberg, 2009. Springer. ISBN 978-3-5402-8257-0.
- [79] René Schenkendorf, Xiangzhong Xie, Moritz Rehbein, Stephan Scholl, and Ulrike Krewer. The impact of global sensitivities and design measures in model-based optimal experimental design. *Processes*, 6(4):27, 2018.
- [80] Jochen Schmid, Philipp Seufert, and Michael Bortz. Adaptive discretization algorithms for locally optimal experimental design. *arXiv preprint arXiv:2406.01541*, 2024.
- [81] A.M. Schweidtmann, E. Esche, A. Fischer, M. Kloft, J. Repke, S. Sager, and A. Mitsos. Machine learning in chemical engineering: A perspective. 93(12):2029–2039, 2021.
- [82] Burr Settles. Active learning literature survey. 2009.
- [83] Wanggang Shen and Xun Huan. Bayesian sequential optimal experimental design for nonlinear models using policy gradient reinforcement learning. *Computer Methods in Applied Mechanics and Engineering*, 416:116304, 2023.
- [84] JD Stigter, D Vries, and KJ Keesman. On adaptive optimal input design: a bioreactor case study. *AIChE journal*, 52(9):3290–3296, 2006.
- [85] Stefan Streif, Felix Petzke, Ali Mesbah, Rolf Findeisen, and Richard D Braatz. Optimal experimental design for probabilistic model discrimination using polynomial chaos. *IFAC Proceedings Volumes*, 47(3):4103–4109, 2014.
- [86] Diego Valderrama, Ana Victoria Ponce-Bobadilla, Sven Mensing, Holger Fröhlich, and Sven Stodtman. Integrating machine learning with pharmacokinetic models: Benefits of scientific machine learning in adding neural networks components to existing PK models. *CPT: Pharmacometrics & Systems Pharmacology*, 13(1):41–53, January 2024.
- [87] Vassilios S Vassiliadis, Walter Kähm, E Antonio del Rio Chanona, and Ye Yuan. *Optimization for Chemical and Biochemical Engineering: theory, algorithms, modeling and applications*. Cambridge University Press, 2021.
- [88] Trung Vu, Evgenia Chunikhina, and Raviv Raich. Perturbation expansions and error bounds for the truncated singular value decomposition. *Linear Algebra and its Applications*, 627:94–139, 2021.
- [89] A. Wächter and L.T. Biegler. On the Implementation of an Interior-Point Filter Line-Search Algorithm for Large-Scale Nonlinear Programming. *Mathematical Programming*, 106(1):25–57, 2006.

- [90] Jialu Wang and Alexander W Dowling. Pyomo. doe: An open-source package for model-based design of experiments in python. *AIChE Journal*, 68(12):e17813, 2022.
- [91] Peiliang Xu. Truncated svd methods for discrete linear ill-posed problems. *Geophysical Journal International*, 135(2):505–514, 1998.
- [92] Qinyu Zhuang, Dirk Hartmann, Hans-J Bungartz, and Juan M Lorenzi. Active-learning-based nonintrusive model order reduction. *Data-Centric Engineering*, 4:e2, 2023.